mathematics

MDPI

Article

An Adaptive Proportional Plus Damping Control for Teleoperation Systems with Asymmetric Time-Varying Communication Delays

Jigang Bao [1,2,†], Liyue Fu [3,*,†], Haochen Zhang [2,4], Ancai Zhang [3], Wenhui Guo [1] and Tiansheng Chen [1]

1 Engineering Training Center, Lanzhou College of Information Science and Technology, Lanzhou 730000, China
2 Gansu Provincial Key Laboratory of Advanced Industrial Process Control, Lanzhou 730050, China
3 School of Automation and Electrical Engineering, Linyi University, Linyi 276000, China
4 College of Electrical and Information Engineering, Lanzhou University of Technology, Lanzhou 730050, China
* Correspondence: fuliyue@outlook.com; Tel.: +86-150-2032-9165
† These authors contributed equally to this work.

Abstract: Communication delay is an important factor affecting the stability and performance of telerobotic systems. In this paper, a new adaptive proportional damping controller is proposed to improve the stability and performance of the system in the presence of the cases such as asymmetric communication delay, unknown gravity torque, friction torque, and other disturbance torques. The proposed proportional damping control method combines the RBF neural network and adaptive control strategy to compensate for the unknown torque. The stability and robustness of the system are enhanced by adding error-damping items, operator force, and environmental force items. The Lyapunov–Krasovskii functional is employed to analyze and prove the exponential stability and signal boundedness of the closed-loop system. The simulation results verify the correctness of the proposed method, and the comparison with the results of other control methods shows the effectiveness of the designed control strategy.

Keywords: teleoperation; proportional damping control; adaptive control; time-varying delay; Lyapunov–Krasovskii function

MSC: 93-10

Citation: Bao, J.; Fu, L.; Zhang, H.; Zhang, A.; Guo, W.; Chen, T. An Adaptive Proportional Plus Damping Control for Teleoperation Systems with Asymmetric Time-Varying Communication Delays. *Mathematics* **2022**, *10*, 4675. https://doi.org/10.3390/math10244675

Academic Editor: Asier Ibeas

Received: 19 November 2022
Accepted: 8 December 2022
Published: 9 December 2022

1. Introduction

In some particular application scenarios, such as nuclear environments, deep sea, space, and industrial environments, there are a lot of demands for operational tasks. However, operators cannot operate in these dangerous and extreme environments, and the present robots are not sufficiently intelligent to work well. Therefore, teleoperation robots have been introduced to perform tasks in various scenarios [1–3].

A typical telerobotic system includes the operator, the master robot, the communication channel, the slave robot, and the task environment [4]. Generally, the control structure of the teleoperation system is the bilateral control scheme. The human operator manipulates the master robot to move, and then the position signals from the master robot are transmitted through a communication channel to the slave side. With the slave controller, the slave robot can track the position of the master robot to perform the task. In addition, positioning signals and/or force signals that interact with the surrounding environment can be transmitted to the master robot, which will act on the master robot and the operator with the action of the master controller.

Stability and positional tracking are the most significant performance objectives for teleoperation systems. In the bilateral teleoperation system, the positional signals are sent through a communication channel and the time delay in communication transmissions is

inevitable. This fact creates an inconsistent factor, i.e., the delay in communication will reduce the performance and stability of the teleoperation system, and may even cause system instability [4,5]. Therefore, since finding the harmfulness of time delay signals to the teleoperation system, many research works have been devoted to analyzing the impact on the system and ensuring its stability of the system.

The passivity theory is the earliest method used to analyze the stability and control performance of time-delay teleoperation. Based on the passive theory, some control methods have been proposed and applied to the control of time-delay teleoperation systems, and good performance of position tracking control has been achieved. Some typical control methods are the scattering approach [6,7] and traditional and improved wave variables [8–11]. The core of the above control methods is to ensure the passivity of the communication, which requires assuming the external forces of the operator and the environment are passive relative to the speed of the robot. However, in practical applications, the passivity assumption of this external force input is conservative and cannot meet the needs of most application scenarios. Therefore, some control methods based on passive theory have limitations in practical applications. In the world, many scholars have proposed and are studying the control methods of time delay teleoperation systems based on the Lyapunov stability theorem. These typical methods include robust control [12], adaptive control based on neural networks and fuzzy systems [13–17], sliding mode control [18–20], output feedback control [21], feedforward-feedback position control [22], observer approach [23], and finite-time control [20]. Among the above methods, the author pays more attention to solving the problem of fixed delay stability of the teleoperation system. However, in practical applications, the changing communication delay in teleoperation systems needs more attention.

Damping injection control is another method to guarantee the stability of the time delay teleoperation system. Its main principle is to use the damping term in the controller to weaken the energy introduced into the system due to time delay. The controller design and stability analysis of the closed-loop system are based on Lyapunov–Krasovskii method. In [24], Nuño proposed a simplified proportional plus damping (P+d) control with constant time delay for the teleoperation system, and rigorous stability proof has also been given. Based on the designed first-order filter, a PD controller without speed measurement is proposed to control the teleoperation system in [25], but the complex communication delay is not fully considered. In [26], Slawinski proposed a compensated P+d control scheme to eliminate energy and realize the good position control performance of the time-delay teleoperation system. The idea of compensation is to consider the simplified model of the operator's behavior before tactile and visual stimuli to modify the instructions. In [27], Islam proposed a new PD control strategy for a teleoperation system with passive and nonpassive input forces, and symmetrical and unsymmetrical time-varying communication delays. In [28], a new P+d-like controller is presented to ensure the position and force tracking control for the network nonlinear teleoperation system. In [29,30], the bilateral position force control strategies based on the P+d method are also designed for the time-delay teleoperation systems, respectively. In [29], the extended active observation filter is designed to measure the external force. In [30], a nonlinear function of environmental forces is added to improve the control performance of the system.

In some research work, the authors consider the influence of torque saturation on the stability and performance of teleoperation systems with time-varying delay and design a P+d control strategy for controller saturation [31,32]. By combining the dynamic master–slave interconnection with the dynamic damping injection of each robot, in [33] the authors propose a new control strategy for the time-delay bilateral teleoperation system with stable input to state. In [34], the authors designed a simplified algorithm with gravity compensation based on traditional P+d control and verified the effectiveness of the algorithm through experiments.

In the above control methods, gravity torque compensation is added to some control laws to achieve better position control performance [35]. However, these algorithms still

ignore the effects of friction torque and external interference torque, and for practical robots, gravity torque may not be accurately obtained, which may weaken the control performance with the above methods. Adaptive control is an effective method and can improve the control performance of complex nonlinear systems with unknown dynamics and disturbances [36,37]. Adaptive control has been widely used in teleoperation systems for position-tracking control. The main principle is to use fuzzy logic systems, radial basis function (RBF) neural networks, and linear parameter models to estimate uncertainties and external disturbances [16,17]. Because of its good characteristics, an adaptive control strategy has been combined with P+d control in some work. In [38], a nonlinear adaptive term of environmental force is added to the slave controller, and a nonlinear proportional plus nonlinear damping (nP+nD) controller is designed. In [39], an adaptive fuzzy logic system is used to estimate and compensate for the uncertain torques, and an improved proportional differential sample plus damping (PD+d) control method is designed.

Therefore, based on the line of analyzing the existing work, this paper focuses on how to combine the RBF neural network, adaptive control method, and P+d control principle to design a novel control strategy to solve the position tracking problem of teleoperation system under the factors of asymmetric time-varying delay, unknown gravity torque, friction torque, and external bounded interference torques. This paper presents a new improved P+d control based on RBF neural network adaptive compensation for teleoperation systems. The fundamental contributions of this paper can be summarized as follows:

- In this paper, a novel control scheme with a proportional plus damping strategy and adaptive compensation is proposed for the time delay teleoperation system. RBF neural network and adaptive control method are employed to estimate and compensate for the unknown torque information.
- The traditional proportional damping injection control is improved to obtain better control performance. The damping term based on position error is introduced to enhance the stability and robustness of the closed-loop system.
- The Lyapunov–Krasovskii functional is used to establish the boundedness and stability of the closed-loop teleoperation system. The relationships between the controller gain coefficients are also given in the stability analysis.

The remainder of this paper is presented as follows. In Section 2, the dynamic descriptions of the teleoperation system and the control problem are described. In Section 3, the proposed adaptive proportional damping injection control scheme is investigated and the stability analysis is also discussed. The simulation experiment results are given in Section 4. Finally, this work is concluded in Section 5.

2. Problem Statement

2.1. Teleoperation System Modeling

Consider the master and slave robots with n degree of freedom (dof) rotation joints, $\boldsymbol{q}_m \in \mathcal{R}^n$, $\boldsymbol{q}_s \in \mathcal{R}^n$, $\dot{\boldsymbol{q}}_m \in \mathcal{R}^n$, $\dot{\boldsymbol{q}}_s \in \mathcal{R}^n$, $\ddot{\boldsymbol{q}}_m \in \mathcal{R}^n$, and $\ddot{\boldsymbol{q}}_s \in \mathcal{R}^n$ are, respectively, defined as the position, velocity, and acceleration vectors of the rotation joints at time $t \in \mathcal{R}^+$. In joint space, the dynamic model equations of the master and slave robots can be described as

$$\begin{aligned} \boldsymbol{M}_m(\boldsymbol{q}_m)\ddot{\boldsymbol{q}}_m + \boldsymbol{C}_m(\dot{\boldsymbol{q}}_m, \boldsymbol{q}_m)\dot{\boldsymbol{q}}_m + \boldsymbol{G}_m(\boldsymbol{q}_m) + \boldsymbol{F}_m &= \boldsymbol{\tau}_m - \boldsymbol{J}_m^T \boldsymbol{F}_h, \\ \boldsymbol{M}_s(\boldsymbol{q}_s)\ddot{\boldsymbol{q}}_s + \boldsymbol{C}_s(\dot{\boldsymbol{q}}_s, \boldsymbol{q}_s)\dot{\boldsymbol{q}}_s + \boldsymbol{G}_s(\boldsymbol{q}_s) + \boldsymbol{F}_s &= \boldsymbol{\tau}_s - \boldsymbol{J}_s^T \boldsymbol{F}_e, \end{aligned} \tag{1}$$

where $\boldsymbol{M}_m(\boldsymbol{q}_m), \boldsymbol{M}_s(\boldsymbol{q}_s) \in \mathcal{R}^{n\times n}$ are the inertia matrices, $\boldsymbol{C}_m(\dot{\boldsymbol{q}}_m, \boldsymbol{q}_m), \boldsymbol{C}_s(\dot{\boldsymbol{q}}_s, \boldsymbol{q}_s) \in \mathcal{R}^{n\times n}$ are the Coriolis and centrifugal matrices, and $\boldsymbol{G}_m(\boldsymbol{q}_m), \boldsymbol{G}_s(\boldsymbol{q}_s) \in \mathcal{R}^n$ are the gravitational torques. $\boldsymbol{F}_m, \boldsymbol{F}_s \in \mathcal{R}^n$ are friction torques and external interference torques. The force exerted by the operator to the end of the master robot is $\boldsymbol{F}_h \in \mathcal{R}^n$, and the environmental force acting on the end of the slave robot is $\boldsymbol{F}_e \in \mathcal{R}^n$. The Jacobian matrices $\boldsymbol{J}_m$ and $\boldsymbol{J}_s$ can map the operator and environment forces to the torques in the joint space of the master and slave robots. The control torques in the master and slave sides are $\boldsymbol{\tau}_m$ and $\boldsymbol{\tau}_s$. Define

$\boldsymbol{X}_m$ and $\boldsymbol{X}_s$ as the end positions of the master and slave manipulators in the Cartesian coordinate system, and $\boldsymbol{X}_m$ and $\boldsymbol{X}_s$ can be obtained through forward kinematics (FK_m and FK_s) of these two robots. The end velocities $\dot{\boldsymbol{X}}_m$ and $\dot{\boldsymbol{X}}_s$ can be calculated through Jacobian matrices and the joint velocities. The above relations are shown in the following

$$\begin{aligned} \boldsymbol{X}_m &= FK_m(\boldsymbol{q}_m), \quad \dot{\boldsymbol{X}}_m = \boldsymbol{J}_m \dot{\boldsymbol{q}}_m, \\ \boldsymbol{X}_s &= FK_s(\boldsymbol{q}_s), \qquad \dot{\boldsymbol{X}}_s = \boldsymbol{J}_s \dot{\boldsymbol{q}}_s. \end{aligned} \tag{2}$$

It is well known that the dynamic models (10) are nonlinear and parameter time-varying. For $j = m, s$, there have some important properties as follows [40,41].

Property 1. *The inertia matrix $\boldsymbol{M}_j(\boldsymbol{q}_j)$ is symmetric positive-definite. In addition, the following inequality relations are satisfied for the maximum eigenvalue $M_{j,max}$ and minimum eigenvalue $M_{j,min}$ of the matrix $\boldsymbol{M}_j(\boldsymbol{q}_j)$*

$$0 < M_{j,min}\boldsymbol{I} \leq \boldsymbol{M}_j(\boldsymbol{q}_j) \leq M_{j,max}\boldsymbol{I} < \infty$$

Property 2. *The matrix $\dot{\boldsymbol{M}}_j - 2\boldsymbol{C}_j$ is a skew-symmetric matrix, which means that for any nonzero vector $\boldsymbol{q} \in \mathcal{R}^n$, the following equation always holds*

$$\boldsymbol{q}^T(\dot{\boldsymbol{M}}_j - 2\boldsymbol{C}_j)\boldsymbol{q} = 0.$$

Property 3. *The gravitational torques $\boldsymbol{G}_m, \boldsymbol{G}_s$, friction torques and external interference torques $\boldsymbol{F}_m, \boldsymbol{F}_s$ are all bounded.*

In a teleoperation system, the position signals of the master and the slave robots need to be transmitted to each other's controllers to form the bilateral control mode. As we all know, the transmission time delay of communication is inevitable. $d_m(t)$ and $d_s(t)$ are employed to represent the communication delay signals from the master side to the slave, and from the slave side to the master side, respectively. Therefore, $\boldsymbol{q}_{sd}$ is defined as the position signal of the master robot transmitted to the slave side, $\boldsymbol{q}_{md}$ is defined as the slave robot position transmitted to the master side, and we have $\boldsymbol{q}_{sd} = \boldsymbol{q}_m(t - d_m(t))$, $\boldsymbol{q}_{md} = \boldsymbol{q}_s(t - d_s(t))$.

Assumption 1. *The asymmetric time-varying communication time delays $d_m(t)$ and $d_s(t)$ are all bounded, and there have two constants $\bar{d}_m \in \mathcal{R}^+$ and $\bar{d}_s \in \mathcal{R}^+$ that*

$$\begin{aligned} 0 \leq d_m(t) \leq \bar{d}_m, \\ 0 \leq d_s(t) \leq \bar{d}_s. \end{aligned}$$

For operator and environmental forces, there has an assumption below

Assumption 2. *The operator force $\boldsymbol{F}_h$ and environment force $\boldsymbol{F}_e$ are also bounded by $\|\boldsymbol{F}_h\| \leq \bar{F}_h$, $\bar{F}_h \geq 0$ and $\|\boldsymbol{F}_e\| \leq \bar{F}_e$, $\bar{F}_e \geq 0$.*

2.2. Control Objectives

For a teleoperation system with asymmetric time-varying delays and bounded operator/environment forces action studied in this work, the main control objective is to design the appropriate master controller and slave controller to build a bilateral control scheme and achieve the closed-loop system satisfies the following performance:

- Stability. The closed-loop system of bilateral teleoperation should be stable, whether under asymmetric time-varying delay or external force.
- Position tracking. The joint positions of the master and slave robots can track each other quickly and with small errors. When the time $t \to \infty$, $\|\boldsymbol{q}(t) - \boldsymbol{q}_s(t)\|$ should approach a small neighborhood of zero or even zero.

2.3. RBF Neural Network

The RBF neural network has been widely employed for the adaptive controller design of the uncertain model system, with the property that it can approximate a nonlinear smooth function with an arbitrary accuracy [42]. In our work, the RBF neural network is used to estimate the unknown gravity torque vector and friction torque vector. The RBF neural network has three layers, namely the input layer, the hidden layer, and the output layer.

For a continuous function $G(x) : \mathcal{R}^a \to \mathcal{R}^b$, $\boldsymbol{x} \in \mathcal{R}^a$ is the input vector, with the RBF neural network, it can be defined as

$$G(x) = \boldsymbol{W}^T \boldsymbol{\varphi}(\boldsymbol{x}) + w. \tag{3}$$

where $\boldsymbol{W} \in \mathcal{R}^{d \times a}$ is the weight matrix, d is the number of network nodes. $\boldsymbol{\varphi} = [\varphi_1, \varphi_2, \ldots, \varphi_d]^T$ is the Gaussian basis function vector and can be calculated as

$$\varphi_i = e^{-\frac{(x-\boldsymbol{b}_i)^T(x-\boldsymbol{b}_i)}{2c^2}}, i = 1, 2, \ldots, d.$$

$\boldsymbol{b}_i \in \mathcal{R}^a$ is the Gaussian center vector of the i-th node. c is the width of the Gaussian function. w is the bounded approximate error.

Remark 1. *In more applications of the RBF network, some methods can be used to obtain center vectors and widths of Gaussian base functions, while the matrix of the coefficient of weight can be obtained through the training of the data. However, it is important to note that in adaptive control methods with the RBF neural network, the weight matrix for neural networks is usually constructed and obtained by the Lyapunov stability criterion. The stability and convergence of the system can be assured by the development of adaptive learning rules. The Gauss-centered vector of i-the node* $\boldsymbol{b}_i$ *is determined concerning a range of input values of the neural network. In addition, input data values of the RBF neural network should be in the effect range of Gaussian functions by giving a suitable width of c.*

3. Adaptive Proportional Plus Damping Control Design

In this subsection, a novel adaptive proportional plus damping control method is described. Firstly, RBF neural network is used to approximate and compensate the unknown parts of gravitational torques $\boldsymbol{G}_m, \boldsymbol{G}_s$, friction torques, and external interference torques $\boldsymbol{F}_m, \boldsymbol{F}_s$, which are expressed as follows

$$\begin{aligned} \boldsymbol{G}_m(\boldsymbol{q}_m) + \boldsymbol{F}_m &= \boldsymbol{W}_m^T \boldsymbol{\varphi}_m(\boldsymbol{x}_m) + \boldsymbol{w}_m, \\ \boldsymbol{G}_s(\boldsymbol{q}_s) + \boldsymbol{F}_s &= \boldsymbol{W}_s^T \boldsymbol{\varphi}_s(\boldsymbol{x}_s) + \boldsymbol{w}_s. \end{aligned} \tag{4}$$

where for $j = m,\ s$, $\boldsymbol{W}_j \in \mathcal{R}^{l \times n}$ is the ideal approximate weight matrix of the RBF neural network with l nodes, $\boldsymbol{x}_j = \left[\boldsymbol{q}_j^T, \dot{\boldsymbol{q}}_j^T\right]^T$ is the input vector of the neural network. $\boldsymbol{\varphi}_j(\boldsymbol{x}_j) \in \mathcal{R}^{l \times 1}$ is the Gaussian basis function vector, which can be calculated by

$$\varphi_{j,i} = e^{-\frac{\left(\boldsymbol{x}_j - \boldsymbol{b}_{j,i}\right)^T \left(\boldsymbol{x}_j - \boldsymbol{b}_{j,i}\right)}{2c_j^2}}, i = 1, 2, \ldots, l. \tag{5}$$

$\boldsymbol{b}_{j,i} \in \mathcal{R}^{1 \times ln}$ is the Gaussian center function vector of the i-th hidden layer node. c_j is the width of the Gaussian function. Then the dynamics of the teleoperation system can be rewritten as

$$\begin{aligned} \boldsymbol{M}_m(\boldsymbol{q}_m)\ddot{\boldsymbol{q}}_m + \boldsymbol{C}_m(\dot{\boldsymbol{q}}_m, \boldsymbol{q}_m)\dot{\boldsymbol{q}}_m + \boldsymbol{W}_m^T \boldsymbol{\varphi}_m(\boldsymbol{x}_m) + \boldsymbol{w}_m &= \boldsymbol{\tau}_m - \boldsymbol{J}_m^T \boldsymbol{F}_h, \\ \boldsymbol{M}_s(\boldsymbol{q}_s)\ddot{\boldsymbol{q}}_s + \boldsymbol{C}_s(\dot{\boldsymbol{q}}_s, \boldsymbol{q}_s)\dot{\boldsymbol{q}}_s + \boldsymbol{W}_s^T \boldsymbol{\varphi}_s(\boldsymbol{x}_s) + \boldsymbol{w}_s &= \boldsymbol{\tau}_s - \boldsymbol{J}_s^T \boldsymbol{F}_e, \end{aligned} \tag{6}$$

As mentioned in [43,44], P+d control is a damping injection control method that can ensure position tracking with varying time delays. In our work, the nonlinear control term of position error and the adaptive compensation term for unknown torque are introduced into the traditional P+d control method, and the following control strategy is constructed

$$\begin{aligned}\boldsymbol{\tau}_m =& -K_{m1}\boldsymbol{\kappa}_m(\boldsymbol{q}_m-\boldsymbol{q}_{sd})^T(\boldsymbol{q}_m-\boldsymbol{q}_{sd})-\boldsymbol{K}_m\dot{\boldsymbol{q}}_m\\ &-\boldsymbol{P}(\boldsymbol{q}_m-\boldsymbol{q}_{sd})+\hat{\boldsymbol{W}}_m\boldsymbol{\varphi}_m(\boldsymbol{x}_m)+\hat{\boldsymbol{w}}_m+\boldsymbol{J}_m^T\boldsymbol{F}_h,\\ \boldsymbol{\tau}_s =& -K_{s1}\boldsymbol{\kappa}_s(\boldsymbol{q}_s-\boldsymbol{q}_{md})^T(\boldsymbol{q}_s-\boldsymbol{q}_{md})-\boldsymbol{K}_s\dot{\boldsymbol{q}}_s\\ &-\boldsymbol{P}(\boldsymbol{q}_s-\boldsymbol{q}_{md})+\hat{\boldsymbol{W}}_s\boldsymbol{\varphi}_s(\boldsymbol{x}_s)+\hat{\boldsymbol{w}}_s+\boldsymbol{J}_s^T\boldsymbol{F}_e.\end{aligned} \tag{7}$$

where for $j=m,\ s$, $K_{j1}>0$ is the gain weight of position error nonlinear control term, $\boldsymbol{K}_j$ is the damping coefficient matrix, $\boldsymbol{P}$ represents the proportional gain matrix. K_{j1} and $\boldsymbol{P}$ are all the positive diagonal gain matrices. $\boldsymbol{\kappa}_j$ is defined as the stability gain vector, which is used to ensure the stability of the system with the action of the position error control item. $\boldsymbol{\kappa}_j=\left[\kappa_{j1},\kappa_{j2},\ldots,\kappa_{jn}\right]^T$ is defined as

$$\kappa_{ji}=\begin{cases}\dfrac{1}{\dot{q}_{ji}},\ if\dot{q}_{ji}\neq 0\\ 0,\ if\dot{q}_{ji}=0\end{cases},\ i=1,\ 2,\ldots,\ n \tag{8}$$

Based on the above definition, we can further obtain that

$$\dot{\boldsymbol{q}}_j^T\kappa_j=\begin{cases}1,\ if\|q_j\|\neq 0\\ 0,\ if\|q_j\|=0\end{cases} \tag{9}$$

Remark 2. *The time-varying communication delay will lead to the disturbance of the position tracking errors $\boldsymbol{q}_m-\boldsymbol{q}_{md}$ and $\boldsymbol{q}_s-\boldsymbol{q}_{sd}$ in the master and slave controllers, which means that the closed-loop system is injected with energy and the stability of the system is weakened. In the traditional damping injection control, the damping term $\boldsymbol{K}_j\dot{\boldsymbol{q}}_j$ is introduced to dissipate and weaken the harmful energy, to ensure the stability of the system. In our work, the introduced position error damping control term is also a damping injection mode. Compared with the traditional mode, the role of the introduced position error damping term can be adjusted according to the position error. The added error damping term increases the energy dissipation of energy introduced by communication delay and enhances the stability and robustness of closed-loop teleoperation. In the controller design, the the stability gain vector $\boldsymbol{\kappa}_j$ calculated by the reciprocal of joint velocity is defined, which not only meets the requirements of damping injection control but also facilitates the analysis of error damping term in stability proof. In addition, a weight coefficient K_{j1} is added to adjust the effect of the error damping term, to prevent oscillation caused by velocity speed and too large position tracking error. Based on this idea, we can also design other forms of error-damping terms to achieve the above analysis functions, such as $k_{j1}sign(\dot{\boldsymbol{q}}_j)(\boldsymbol{q}_j-\boldsymbol{q}_{j'd})^T(\boldsymbol{q}_j-\boldsymbol{q}_{j'd})$, for $j=m,\ s$ and $j'=s,\ m$. The subsequent analysis of this paper only focuses on the control law proposed above, while the stability analysis of other damping term forms is similar.*

Remark 3. *In the above control law, the adaptive control strategy and RBF neural network are introduced to compensate for unknown gravity torque, friction torque, and other unknown bounded disturbance torque. The essence of adaptive control is to design an appropriate adaptive learning law based on Lyapunov theory to ensure the convergence and passivity of the parameter estimation process. The passivity and stability of the closed-loop teleoperation system can be improved to a certain extent by introducing adaptive methods. In this paper, the following forms of adaptive learning laws are designed based on the Lyapunov stability theory. The specific analysis process can refer to the following part of system stability analysis.*

$$\begin{aligned}\dot{\hat{\boldsymbol{W}}}_j &= -\frac{1}{\Lambda_{j1}}\boldsymbol{\varphi}_j^T\dot{\boldsymbol{q}}_j - \frac{1}{K_{j2}}\hat{\boldsymbol{W}}_j,\\ \dot{\hat{\boldsymbol{w}}}_j &= -\frac{1}{\Lambda_{j2}}\dot{\boldsymbol{q}}_j - \frac{1}{K_{j3}}\hat{\boldsymbol{w}}_j.\end{aligned} \tag{10}$$

where Λ_{j1}, Λ_{j2}, K_{j2}, and K_{j3} are the gain coefficients of adaptive learning laws, both of which are positive constants. The control block diagram of the closed-loop teleoperation system is shown in Figure 1.

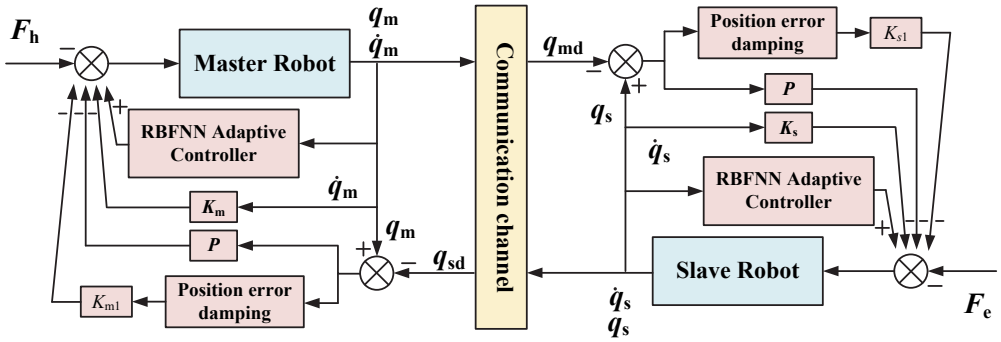

Figure 1. The control block diagram of the teleoperation.

The following theorem serves as a design method and stability for controller (6) for teleoperation systems with asymmetric time-varying delays and unknown gravity, friction, and external torques.

Theorem 1. *In the bilateral teleoperation system in (1) with the control laws in (7) and adaptive laws in (10), the closed-loop system is stable and $\dot{\boldsymbol{q}}_m$, $\dot{\boldsymbol{q}}_s$, and $\boldsymbol{q}_m - \boldsymbol{q}_s$ are bounded for bounded asymmetric time-varying communication delays and unknown gravity, friction, and external torques, respectively. If there exists positive controller gain coefficients K_{j1}, K_{j2}, K_{j3}, Λ_{j1}, and Λ_{j2}, and positive definite control gain matrices $\boldsymbol{K}_j$ and $\boldsymbol{P}$, $j = m,\ s$, and there exist the positive definite skew-symmetric matrix $\boldsymbol{Q}_m$ and $\boldsymbol{Q}_s$, so that the above gain matrices and gain coefficients can satisfy that the new matrices $\boldsymbol{\Gamma}$, $\boldsymbol{\Psi}_j$, and $\boldsymbol{\Psi}_s$ defined below are all positive semidefinite.*

$$\begin{aligned}\boldsymbol{\Gamma} &= K_{m1}\boldsymbol{I} - \frac{\bar{d}_s}{1-\lambda}\boldsymbol{Q}_s^{-1} + K_{s1}\boldsymbol{I} - \frac{\bar{d}_m}{1-\lambda}\boldsymbol{Q}_m^{-1}\\ \boldsymbol{\Psi}_m &= \boldsymbol{K}_m - \bar{d}_m\boldsymbol{Q}_m - \frac{\bar{d}_s}{4\lambda}\boldsymbol{P}\boldsymbol{Q}_s^{-1}\boldsymbol{P}^T\\ \boldsymbol{\Psi}_s &= \boldsymbol{K}_s - \bar{d}_s\boldsymbol{Q}_s - \frac{\bar{d}_m}{4\lambda}\boldsymbol{P}\boldsymbol{Q}_m^{-1}\boldsymbol{P}^T\end{aligned} \tag{11}$$

The detailed proof process of Theorem 1 can be seen in Appendix B.

4. Simulation Results

The system used in the simulation is a pair of two manipulators with 2-dof revolute joints. The asymmetry varying time delays, unknown gravity and friction torques, and the external forces of the operator and the environment are also taken into account. The principle block diagram of the simulation experiment is shown in Figure 2.

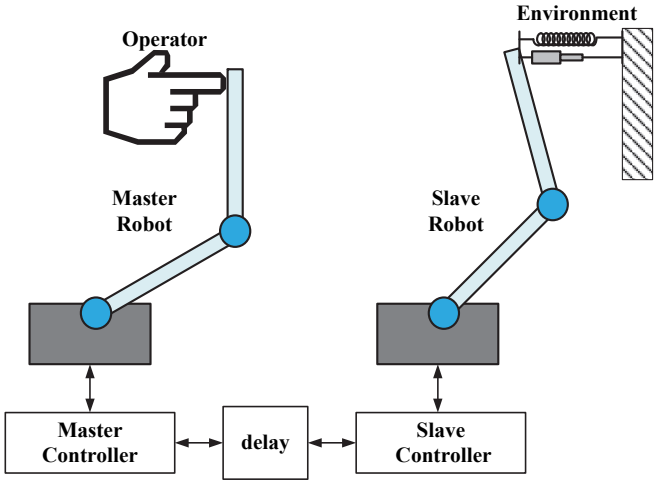

Figure 2. The block diagram of the simulation experiment.

The teleoperation system used for simulation consists of two robot manipulators with 2-dof revolute joints. The asymmetric time-varying delays, uncertain dynamics, and external operator/environment forces are also considered in the simulation experiments. The dynamics of the master and remote robots are similar to (1), where the inertia matrix $\boldsymbol{M}_j$, centripetal Coriolis matrix $\boldsymbol{C}_j$, gravitational torque $\boldsymbol{G}_j$, and friction torque $\boldsymbol{F}_j$ in actual robot dynamics are defined as [41]

$$\boldsymbol{M}_j = \begin{bmatrix} m_{j11} & m_{j12} \\ m_{j21} & m_{j22} \end{bmatrix}, \qquad \boldsymbol{C}_j = \begin{bmatrix} c_{j11} & c_{j12} \\ c_{j21} & c_{j22} \end{bmatrix},$$
$$\boldsymbol{G}_j = \begin{bmatrix} g_{j1}, g_{j2} \end{bmatrix}^{\mathrm{T}}, \qquad \boldsymbol{F}_j = \begin{bmatrix} f_{j1}, f_{j2} \end{bmatrix}^{\mathrm{T}}.$$

The elements of the above matrices $\boldsymbol{M}_j$, $\boldsymbol{C}_j$, $\boldsymbol{G}_j$, and $\boldsymbol{F}_j$ can be described as $m_{j11} = l_{j1}^2(m_{j1} + m_{j2}) + l_{j2}m_{j2}(2l_{j1}\cos q_{j2} + l_{j2})$, $m_{j12} = m_{j21} = l_{j2}^2 m_{j2} + l_{j1}l_{j2}m_{j2}\cos q_{j2}$, $m_{22} = l_{j2}^2 m_{j2}$, $c_{11} = -l_{j1}l_{j2}m_{j2}\sin q_{j2}\dot{q}_{j2}$, $c_{12} = -l_{j1}l_{j2}m_{j2}\sin q_{j2}(\dot{q}_{j1} + \dot{q}_{j2})$, $c_{21} = l_{j1}l_{j2}m_{j2}\sin q_{j2}$, $c_{22} = 0$, $g_{j1} = (m_{j1} + m_{j2})l_{j1}g\cos(q_{j1}) + m_{j2}l_{j2}g\cos(q_{j1} + q_{j2})$, $g_{j2} = m_{j2}l_{j2}g\cos(q_{j1} + q_{j2})$, $f_{j1} = 0.5\dot{q}_{j1} + 0.2\mathrm{sign}(\dot{q}_{j1})$, and $f_{j2} = 0.5\dot{q}_{j2} + 0.2\mathrm{sign}(\dot{q}_{j2})$. For simplicity, the configuration parameters of the teleoperation system are represented in Table 1 [38].

Table 1. Physical parameters of the teleoperation system.

m_{m1}	m_{m2}	l_{m1}	l_{m2}	m_{s1}	m_{s2}	l_{s1}	l_{s2}
4.0 kg	0.5 kg	1.0 m	1.0 m	3.4 kg	0.25 kg	1.0 m	1.0 m

In the simulation experiment, the asymmetric time-varying communication delays at the master and slave sides are shown in Figure 3. The force interactions between the robot and the operator and the environment are all assumed to be the stiffness-damping models. Therefore, the operator input force $\boldsymbol{F}_h$ and environmental force $\boldsymbol{F}_e$ are modeled as follows

$$\begin{aligned} \boldsymbol{F}_h &= \boldsymbol{f}_h + b_h\dot{\boldsymbol{X}}_m + k_h(\boldsymbol{X}_m - \boldsymbol{x}_{m0}), \\ \boldsymbol{F}_e &= b_e\dot{\boldsymbol{X}}_s + k_e(\boldsymbol{X}_s - \boldsymbol{x}_{s0}). \end{aligned}$$

where $\boldsymbol{f}_h$ is the external operator force, its curve is shown in Figure 4, it can be seen that the operator exerts the additional trapezoidal forces in x and y direction from 2 s to 8 s. b_h and k_h are the damping and stiffness coefficients of the operator force dynamic respectively. b_e and k_e are the damping and stiffness coefficients of the environment force model. $\boldsymbol{x}_{m0}$ and $\boldsymbol{x}_{s0}$ represent the initial position points of the force applied by the operator and the

environment, respectively. In this simulation experiment, $k_h = k_e = 10\ N/m$, $b_h = 2\ N/(m/s)$, $b_e = 2.5\ N/(m/s)$, $\boldsymbol{x}_{m0} = [0.707, 1.707]^T m$, and $\boldsymbol{x}_{s0} = [0.5, 0.866]^T m$.

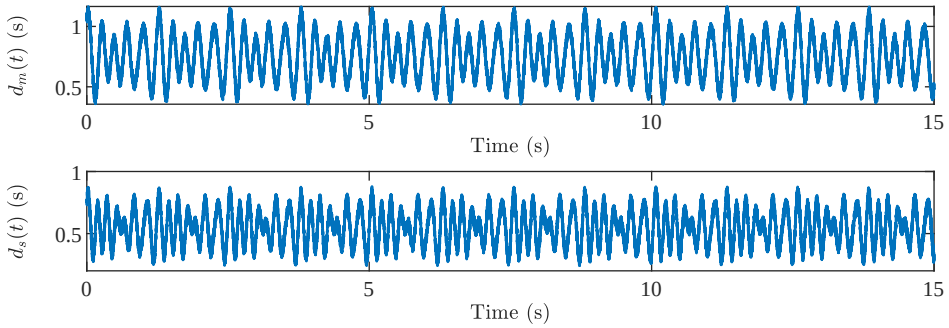

Figure 3. Forward and backward time varying delays d_m and d_s.

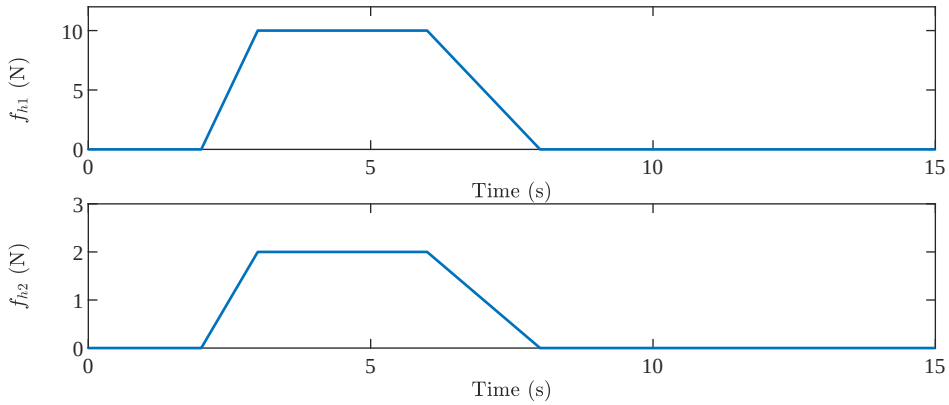

Figure 4. External operator forces $\boldsymbol{F}_h$ in the x-direction and y-direction.

The adaptive law parameters are set as $\Lambda_{m1} = \Lambda_{m2} = 1$, $\Lambda_{s1} = \Lambda_{s2} = 1$, $K_{m2} = K_{m3} = 1$, and $K_{s2} = K_{s3} = 1$. The gain matrices of the control laws are set as $\boldsymbol{K}_m = \boldsymbol{K}_s = 10\boldsymbol{I}$, $\boldsymbol{P} = 5\boldsymbol{I}$ and the gain parameters $K_{m1} = K_{s1} = 0.1$. The initial joint position of the master robot is $\boldsymbol{q}_{m0} = [\pi/4, \pi/4]^T$, the initial joint position of the slave robot is $\boldsymbol{q}_{s0} = [\pi/3, \pi/4]^T$. The initial joint velocities $\dot{\boldsymbol{q}}_{m0}$ and $\dot{\boldsymbol{q}}_{s0}$ are zeros.

We set up two parts of the simulation experiment to verify and illustrate the stability and effectiveness of the closed-loop system. The simulation experiments are carried out under the MATLAB/Simulink platform.

Firstly, the simulation with our proposed control scheme is considered. The simulation is carried out according to the experimental conditions and controller parameters stated above. This part of the simulation focuses on verifying the stability of the system and the boundedness of the parameters. The results of the simulation are shown in Figures 5–9, respectively.

Figures 5 and 6 represent the joint position tracking performances of master and slave robots. From the joint position and the joint tracking error curves, it can be seen that the master and slave robots achieve position tracking control within about 5 s, and the position tracking errors of the two joints are very small and approach 0. These results prove that the proposed method has a good performance of master-slave robot position tracking control, and the closed-loop system is stable.

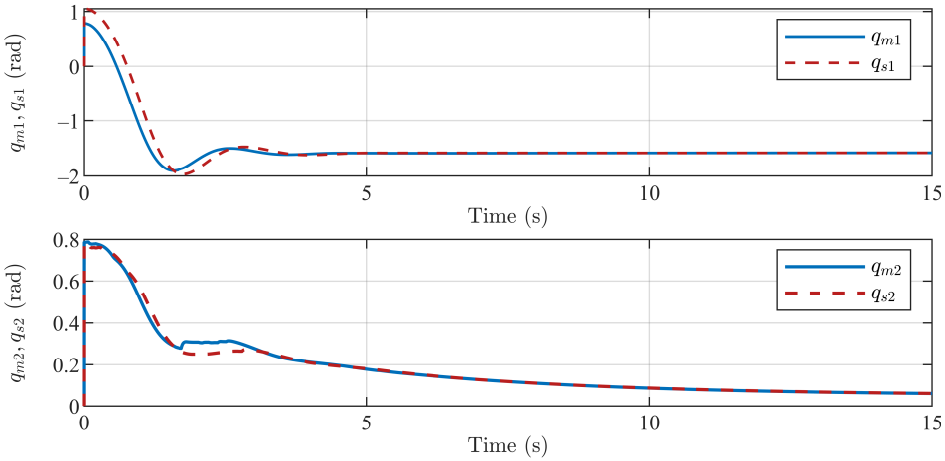

Figure 5. Joint positions of the master and slave end-effectors in the x-direction and y-direction.

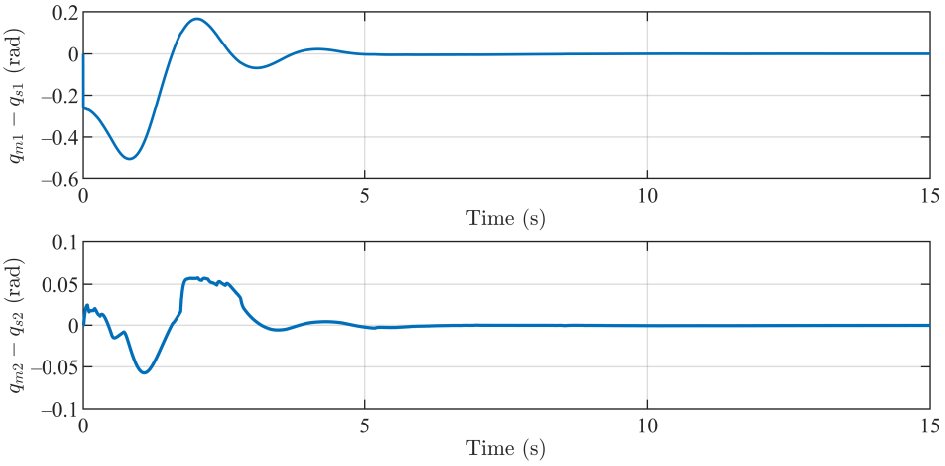

Figure 6. Joint tracking errors of the master and slave robots.

Figure 7 shows the motion of the two links of the master and slave robots in the task space. The red lines present the initial link position and pose of the master and the slave robots. The blue lines indicate the link position and pose of the master and slave robots. The orange lines represent the position of the links between the starting time and the ending time of the master and slave robots. It can be seen that the starting positions of the master and slave robots are different, but with the performances of the controller, external operator force, and environmental force, the ending positions are the same, and the whole moving process is stable.

Figures 8 and 9 show the curves of adaptive parameters $\hat{\boldsymbol{W}}_m$, $\hat{\boldsymbol{W}}_s$, $\hat{w}_m$, and $\hat{\dot{w}}_m$. It can be seen that the adaptive parameters are convergent and bounded in the control process. These results verify that the closed-loop teleoperation system with the proposed method is stable, and the signals of the system are also bounded and convergent.

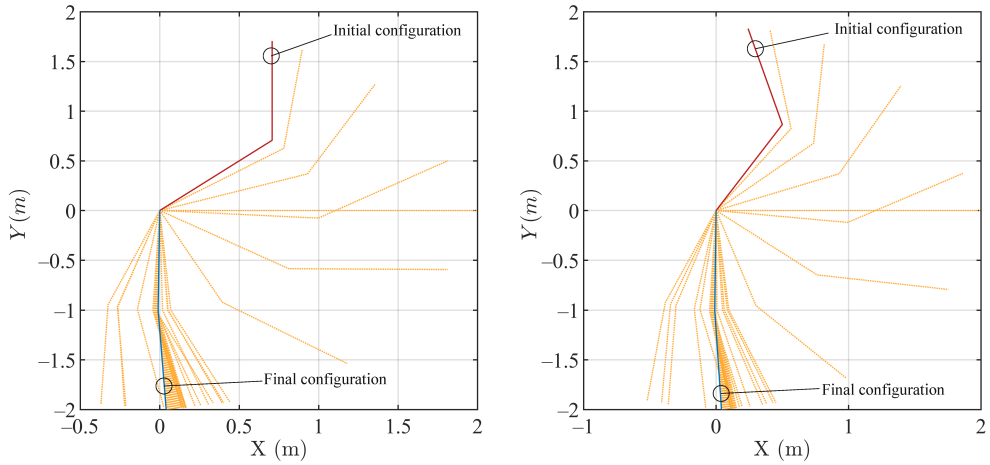

Figure 7. Task performances of the master and slave robots.

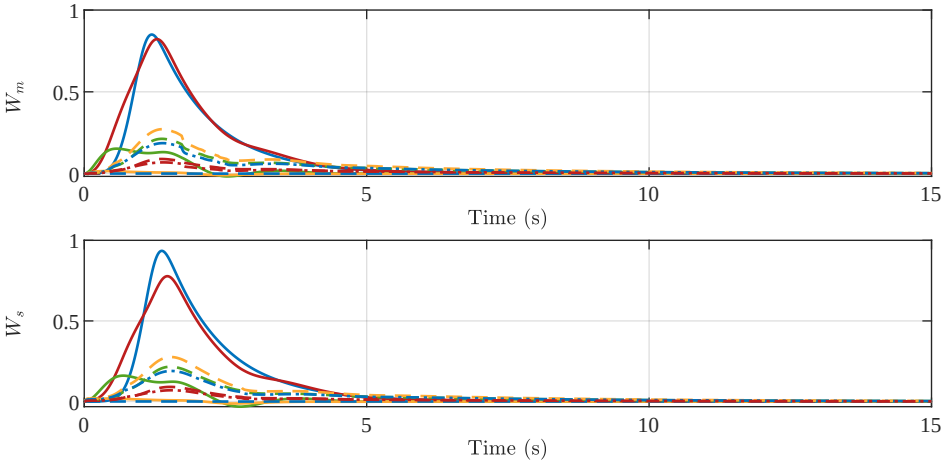

Figure 8. Adaptive parameters in the RBF neural networks $\hat{W}_m$ and $\hat{W}_s$.

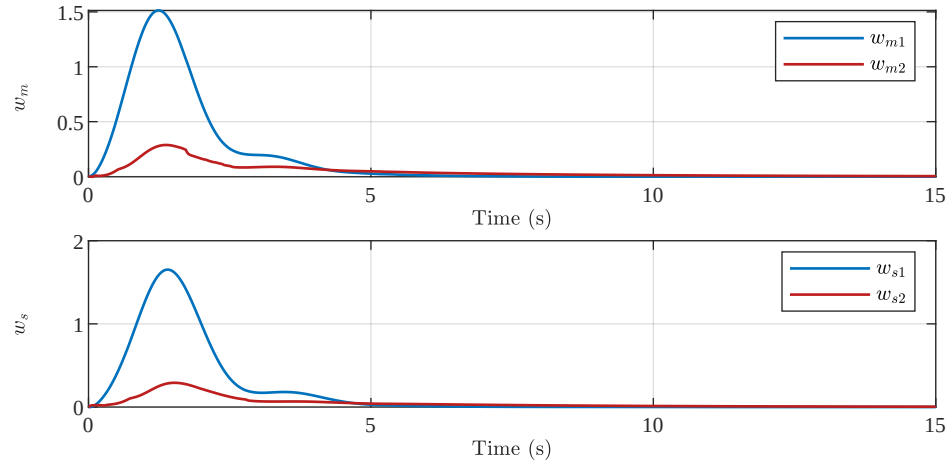

Figure 9. Adaptive parameters of $\hat{w}_m$ and $\hat{w}_s$.

In the second part of the simulation, we selected some representative damping injection control work, implemented these control methods in the simulation, and compared the results of these methods with the proposed methods to verify the effectiveness of the methods presented in this paper. Three cases based on three different damping injection control methods are set. Case 1: in [34], the authors proposed a simplified but classical proportional damping injection control method with gravity compensation. Case 2 [38]: with

the traditional proportional damping injection control, the author added an adaptive part based on parameter linearization to compensate for the gravity torque. This idea is similar to our work, but the difference is that the position error damping term is not introduced into the control scheme. Case 3 [39]: the author designed a proportional differential plus damping injection method, which has no gravity torque compensation and operating force and environmental force feedback in the control law. The detailed simulation results and results comparison are shown in Figures 10–18.

Figures 10 and 11 show the joint position tracking curves and the motion performance in the workspace of the master and slave robots based on the Case 1 method. It can be seen that the position tracking performances of the master and slave robots have entered into the stable state within 10 s, and there is a certain amount of steady-state errors. The joint position error results in Case 1 are compared with the error results of the proposed method, as shown in Figure 12. The simulation experimental conditions are the same as those above. It can be clearly seen that the position tracking performance with Case 1 is affected by additional operator forces due to the lack of friction torque and operator force compensation, and the convergence speed is slow. The proposed method has faster convergence speed and smaller steady-state errors.

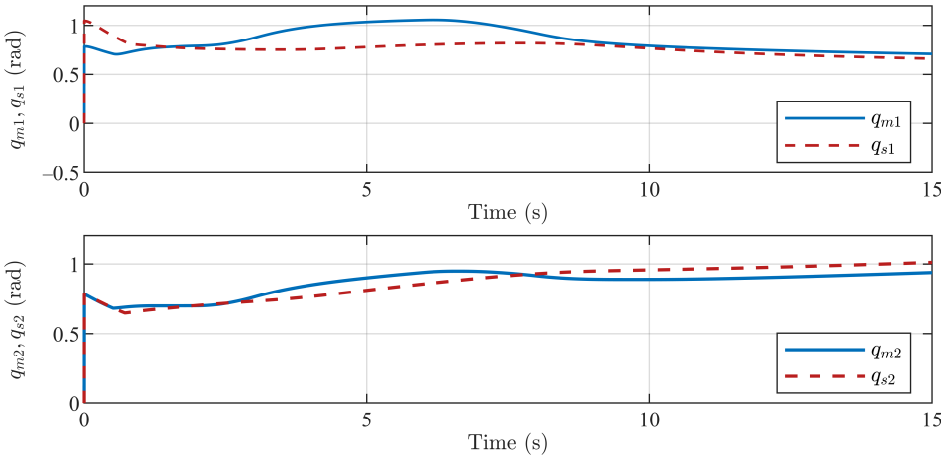

Figure 10. Joint positions of the master and slave end-effectors with the method in Case 1.

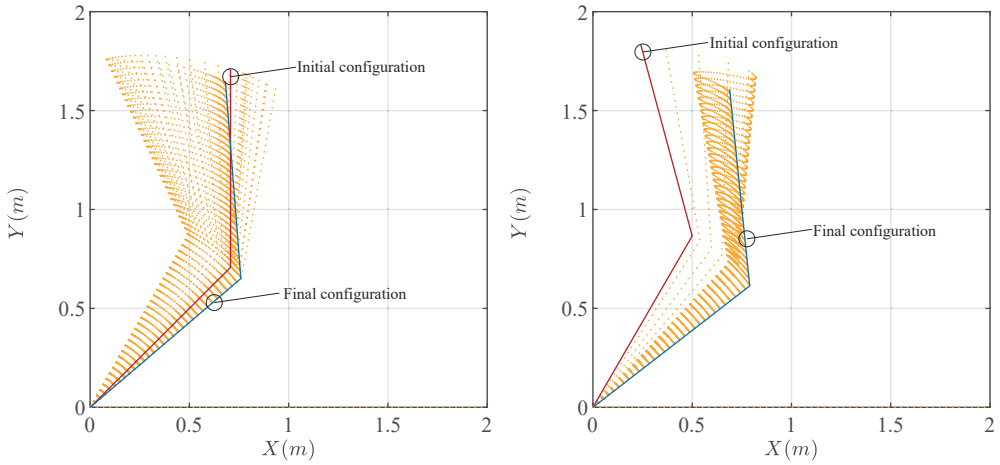

Figure 11. Task performances of the master and slave robots with the method in Case 1.

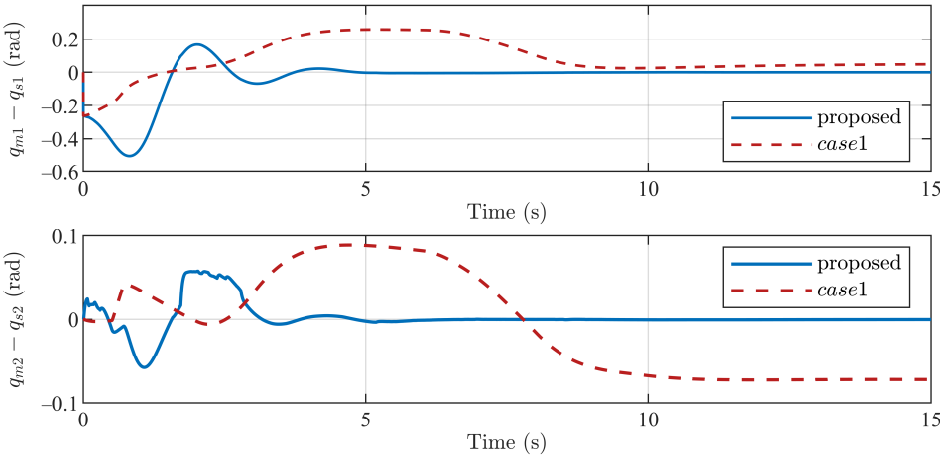

Figure 12. Comparisons of joint tracking errors based on the proposed method and the method in Case 1.

Figures 13 and 14 show the joint position tracking and the task performance of the master and slave robots based on the method in Case 2. It is shown that the joint position tracking the performance of the master and slave robots is not affected by the additional operator force with the adaptive control, operator, and environment force compensation. The position tracking errors can approach a very small range within a certain time, and the task performance does not have a process of vibration. Similarly, the error tracking results of the method in Case 2 are compared with the results of the proposed method. It can be seen that the error convergence speed of Case 2 is slower, and the convergence error of joint 2 is larger. The proposed method has advantages in position tracking performance.

Figures 16 and 17 show the joint position tracking and the task performance of the master and slave robots based on the method in Case 3. It can be seen that the introduction of a differential term in Case 3 improves the convergence speed. Under the adaptive compensation of the fuzzy system, the first joint position tracking error converges quickly and the steady-state error is small, but the second joint position tracking error is large. The task performances also illustrate the above issues. Figure 1 shows the comparison between the joint position tracking errors using the Case 3 method and the proposed method. The control method in Case 3 has a faster convergence speed, but the position tracking accuracy is not as good as the proposed control method.

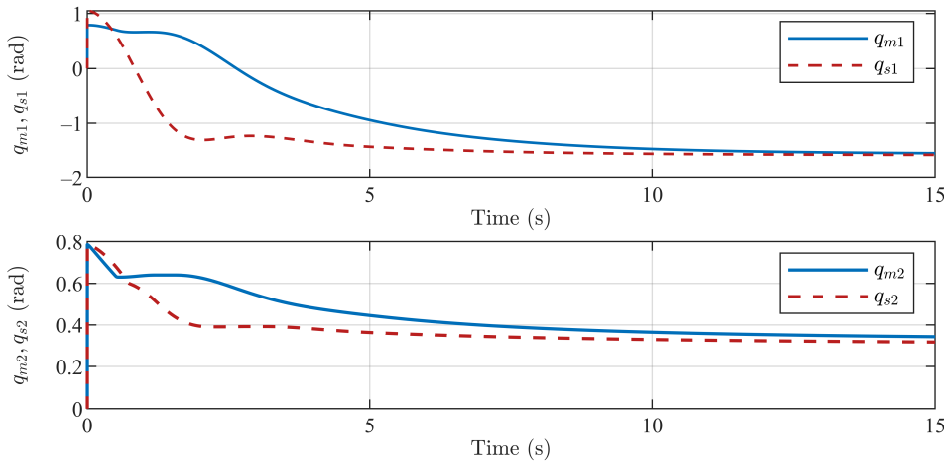

Figure 13. Joint positions of the master and slave end-effectors with the method in Case 2.

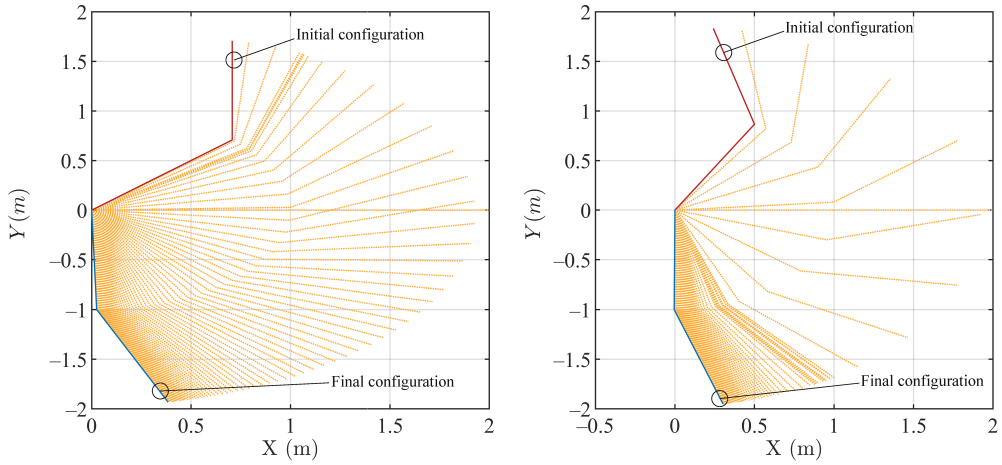

Figure 14. Task performances of the master and slave robots with the method in Case 2.

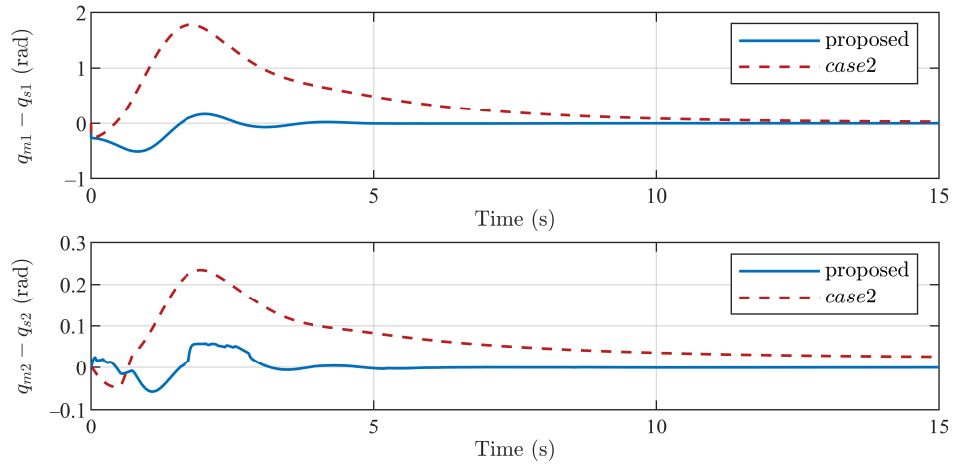

Figure 15. Comparisons of Joint tracking errors based on the proposed method and the method in Case 2.

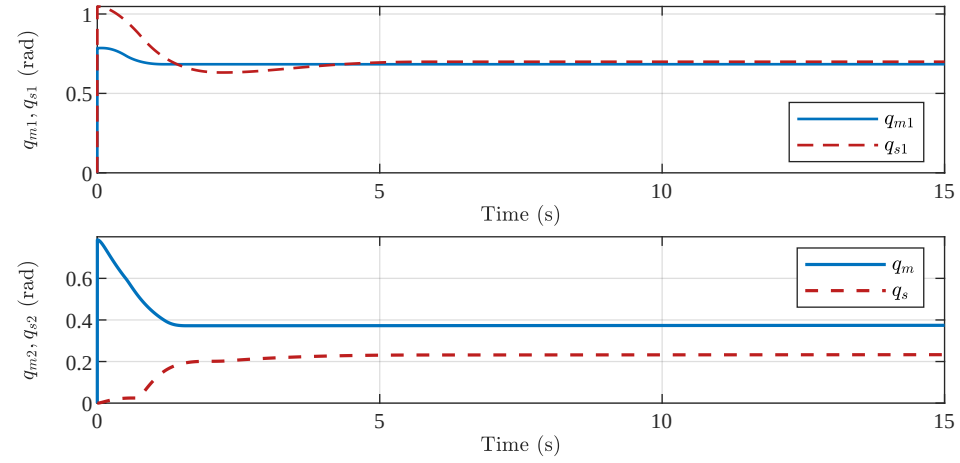

Figure 16. Joint positions of the master and slave end-effectors with the method in Case 3.

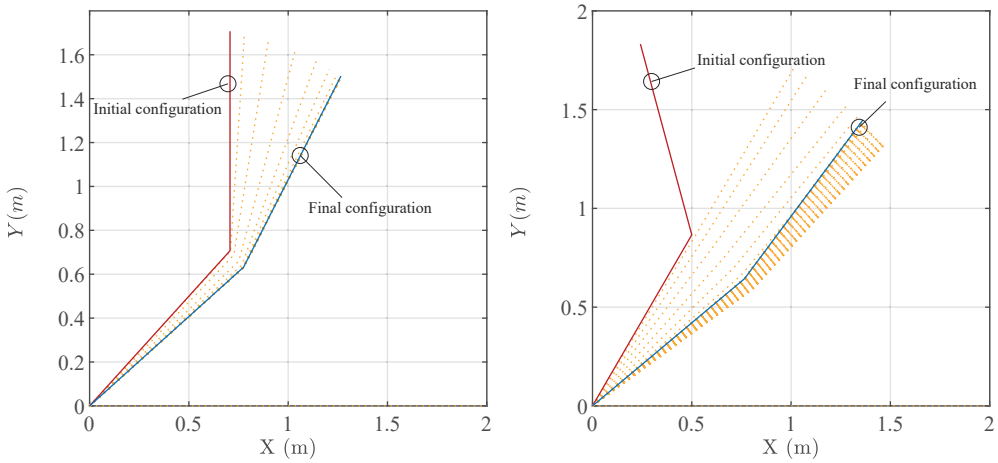

Figure 17. Task performances of the master and slave robots with the method in Case 3.

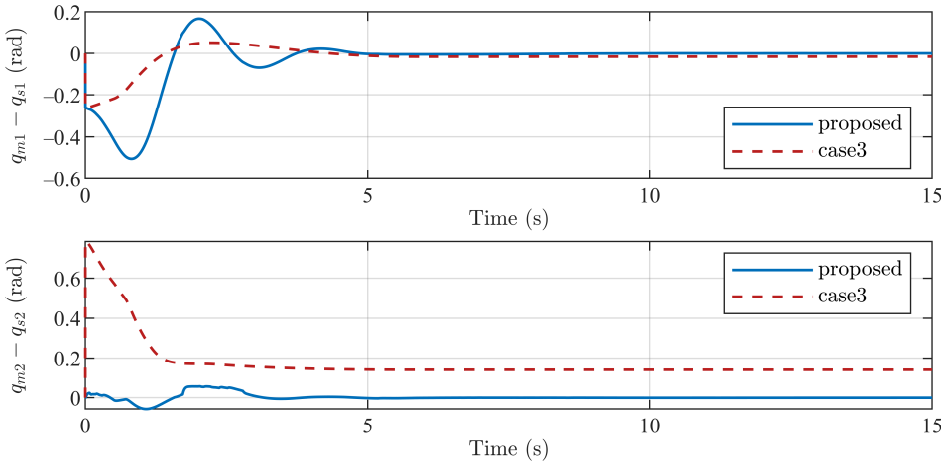

Figure 18. Comparisons of task space tracking errors based on the proposed method and the method in Case 3.

Based on the above analysis of the position tracking performance of these three damping injection control methods in Case 1, Case 2, and Case 3, it further illustrates that the proposed control scheme has advantages in position tracking accuracy and is superior to Case 1 and Case 2 in convergence speed.

5. Conclusions

This paper presents a new adaptive proportional damping injection control method for teleoperation systems, which considers the existence of asymmetric time-varying time delay, unknown gravity torque, friction torque, and disturbance torque. The stability of the time-delay system is further enhanced by introducing the position error damping term. The RBF neural network and adaptive control method are used to compensate for the unknown torque information. A Lyapunov–Krasovskii function is defined for the stability analysis of the closed-loop teleoperation system. The verification simulation of the proposed method and the comparison simulation with the results of other control methods are implemented, respectively. In the verification simulation, the position information of the master and slave robots could enter a stable state with very small errors of about 5 s. In the comparative simulation, the proposed method has the advantages in the steady state errors of position tracking and the rapidity of convergence. The proposed adaptive P+d method can be used for telemedicine and teleoperation of mobile robots [45]. We also plan to apply the method proposed in this paper to industrial robot systems. However, it should be noted that the position error damping term introduced in this paper has singular characteristics near zero velocity, which will bring oscillation to the control value. In addition, avoiding oscillation

near a singular value, introducing the idea of robust control into the controller design, and carrying out some physical experiments to verify the proposed method are also the directions of our future research and need to be further carried out.

Author Contributions: Methodology, J.B. and L.F.; Formal analysis, H.Z.; Investigation, A.Z., W.G. and T.C.; Data curation, J.B.; Writing—original draft, J.B. and L.F.; Writing—review and editing, H.Z. and A.Z.; Project administration, L.F.; Funding acquisition, L.F. and H.Z. All authors have read and agreed to the published version of the manuscript.

Funding: This research was funded by the National Natural Science Foundation of China (No. 62203196), Natural Science Foundation Program of Shandong Province (No. ZR2022QF121 and No. ZR2019YQ28), Gansu Education Science and Technology Innovation Fund Project (No. 2022A-021), Natural Science Foundation Program of Gansu Province (No. 22JR5RA272), Open Fund Project of Gansu Provincial Key Laboratory of Industrial Process Advanced Control (No. 2022KX03), and Basic Scientific Research Project of Southeast University (No. 2242022K30056).

Data Availability Statement: Not applicable.

Conflicts of Interest: The authors declare no conflict of interest.

Appendix A. Preliminary Lemmas

In order to better analyze the stability of the closed-loop system, some useful lemmas are introduced here.

Lemma A1 ([46]). *For a positive-definite matrix $\boldsymbol{Q} \in \mathcal{R}^{n\times n}$ and arbitrary vectors related to time t $\boldsymbol{X}(t) \in \mathcal{R}^n$ and $\boldsymbol{Y}(t) \in \mathcal{R}^n$, the following inequation always holds as:*

$$\pm \boldsymbol{X}^T(t) \int_{t-d(t)}^{t} \boldsymbol{Y}(\xi) d\xi - \int_{t-d(t)}^{t} \boldsymbol{Y}^T(\xi) \boldsymbol{Q} \boldsymbol{Y}(\xi) d\xi \leq \frac{\bar{d}}{4} \boldsymbol{X}^T(t) \boldsymbol{Q}^{-1} \boldsymbol{X}(t) \tag{A1}$$

where $0 \leq d(t) \leq \bar{d}$.

Lemma A2 ([47]). *Let there be two continuous and differentiable time functions $f(t)$ and $V(t)$: $[0, +\infty) \in \mathcal{R}$, for any time $t : t \geq t_0 \geq 0$ and constant $\alpha \in \mathcal{R}^+$, if $\dot{V} \leq -\alpha V + f$, the following inequality is always true.*

$$V(t) \leq e^{-\alpha(t-t_0)} V(t_0) + \int_{t_0}^{t} e^{-\alpha(t-\tau)} f(\tau) d\tau \tag{A2}$$

Appendix B. Proof of Theorem 1

Proof. The proof of this theorem is investigated using the following Lyapunov–Krasovskii function $V = V_1 + V_2 + V_3 + V_4$, where

$$\begin{aligned}
V_1 &= \frac{1}{2} \dot{\boldsymbol{q}}_m^T \boldsymbol{M}_m \dot{\boldsymbol{q}}_m + \frac{1}{2} \dot{\boldsymbol{q}}_s^T \boldsymbol{M}_s \dot{\boldsymbol{q}}_s, \\
V_2 &= \frac{1}{2} (\boldsymbol{q}_m - \boldsymbol{q}_s)^T \boldsymbol{P} (\boldsymbol{q}_m - \boldsymbol{q}_s), \\
V_3 &= \int_{-\bar{d}_m}^{0} \int_{t+\theta}^{t} \dot{\boldsymbol{q}}_m^T(\xi) \boldsymbol{Q}_m \dot{\boldsymbol{q}}_m(\xi) d\xi d\theta + \int_{-\bar{d}_s}^{0} \int_{t+\theta}^{t} \dot{\boldsymbol{q}}_s^T(\xi) \boldsymbol{Q}_s \dot{\boldsymbol{q}}_s(\xi) d\xi d\theta \\
V_4 &= \frac{\Lambda_{m1}}{2} \mathrm{tr}\left(\widetilde{\boldsymbol{W}}_m^T \widetilde{\boldsymbol{W}}_m \right) + \frac{\Lambda_{m2}}{2} \widetilde{\boldsymbol{w}}_m^T \widetilde{\boldsymbol{w}}_m + \frac{\Lambda_{s1}}{2} \mathrm{tr}\left(\widetilde{\boldsymbol{W}}_s^T \widetilde{\boldsymbol{W}}_s \right) + \frac{\Lambda_{s2}}{2} \widetilde{\boldsymbol{w}}_s^T \widetilde{\boldsymbol{w}}_s.
\end{aligned} \tag{A3}$$

V_1 represents the total kinetic energy of the master robot and slave robot; V_2 represents the potential energy in proportional control; V_3 characterizes the energy of forward and backward communication channels with time-varying delay; V_4 represents the energy of adaptive estimation.

With the property of the system in Property 2 and the control laws in (7), the derivative of V_1 is computed as

$$\begin{aligned}\dot{V}_1 =& -K_{m1}(\boldsymbol{q}_m-\boldsymbol{q}_{sd})^T(\boldsymbol{q}_m-\boldsymbol{q}_{sd})\boldsymbol{I}-\dot{\boldsymbol{q}}_m^T\boldsymbol{K}_m\dot{\boldsymbol{q}}_m-\dot{\boldsymbol{q}}_m^T\boldsymbol{P}(\boldsymbol{q}_m-\boldsymbol{q}_{sd})\\&+\dot{\boldsymbol{q}}_m^T\left(\widetilde{\boldsymbol{W}}_m^T\boldsymbol{\varphi}_m+\widetilde{\boldsymbol{w}}_m\right)-K_{s1}(\boldsymbol{q}_s-\boldsymbol{X}_{md})^T(\boldsymbol{q}_s-\boldsymbol{q}_{md})\boldsymbol{I}-\dot{\boldsymbol{q}}_s^T\boldsymbol{K}_s\dot{\boldsymbol{q}}_s\\&-\dot{\boldsymbol{q}}_s^T\boldsymbol{P}(\boldsymbol{q}_s-\boldsymbol{q}_{md})+\dot{\boldsymbol{q}}_s^T\left(\widetilde{\boldsymbol{W}}_s^T\boldsymbol{\varphi}_s+\widetilde{\boldsymbol{w}}_s\right)\end{aligned}\tag{A4}$$

For terms $(\boldsymbol{q}_m-\boldsymbol{q}_{sd})^T(\boldsymbol{q}_m-\boldsymbol{q}_{sd})$ and $(\boldsymbol{q}_s-\boldsymbol{q}_{md})^T(\boldsymbol{q}_s-\boldsymbol{q}_{md})$, based on the definition of integral, the following inequalities exist

$$\begin{aligned}(\boldsymbol{q}_m-\boldsymbol{q}_{sd})^T(\boldsymbol{q}_m-\boldsymbol{q}_{sd})\geq&(\boldsymbol{q}_m-\boldsymbol{q}_s)^T(\boldsymbol{q}_m-\boldsymbol{q}_s)+2(\boldsymbol{q}_m-\boldsymbol{q}_s)^T\int_{t-d_s}^{t}\dot{\boldsymbol{q}}_s(\xi)d\xi,\\(\boldsymbol{q}_s-\boldsymbol{q}_{md})^T(\boldsymbol{q}_s-\boldsymbol{q}_{md})\geq&(\boldsymbol{q}_s-\boldsymbol{q}_m)^T(\boldsymbol{q}_s-\boldsymbol{q}_m)+2(\boldsymbol{q}_s-\boldsymbol{q}_m)^T\int_{t-d_m}^{t}\dot{\boldsymbol{q}}_m(\xi)d\xi\end{aligned}\tag{A5}$$

Then, it can be obtained as

$$\begin{aligned}\dot{V}_1\leq&-K_{m1}(\boldsymbol{q}_m-\boldsymbol{q}_s)^T(\boldsymbol{q}_m-\boldsymbol{q}_s)\boldsymbol{I}-\dot{\boldsymbol{q}}_m^T\boldsymbol{K}_m\dot{\boldsymbol{q}}_m-\dot{\boldsymbol{q}}_m^T\boldsymbol{P}(\boldsymbol{q}_m-\boldsymbol{q}_{sd})\\&+\dot{\boldsymbol{q}}_m^T\left(\widetilde{\boldsymbol{W}}_m^T\boldsymbol{\varphi}_m+\widetilde{\boldsymbol{w}}_m\right)-2(\boldsymbol{q}_m-\boldsymbol{q}_s)^T\int_{t-d_s}^{t}\dot{\boldsymbol{q}}_s(\xi)d\xi\\&-K_{s1}(\boldsymbol{q}_s-\boldsymbol{q}_m)^T(\boldsymbol{q}_s-\boldsymbol{q}_m)\boldsymbol{I}-\dot{\boldsymbol{q}}_s^T\boldsymbol{K}_s\dot{\boldsymbol{q}}_s-\dot{\boldsymbol{q}}_s^T\boldsymbol{P}(\boldsymbol{q}_s-\boldsymbol{q}_{md})\\&+\dot{\boldsymbol{q}}_s^T\left(\widetilde{\boldsymbol{W}}_s^T\boldsymbol{\varphi}_s+\widetilde{\boldsymbol{w}}_s\right)-2(\boldsymbol{q}_s-\boldsymbol{q}_m)^T\boldsymbol{B}_s\int_{t-d_m}^{t}\dot{\boldsymbol{q}}_m(\xi)d\xi.\end{aligned}\tag{A6}$$

where $\widetilde{\boldsymbol{W}}_m$, $\widetilde{\boldsymbol{W}}_s$, $\widetilde{\boldsymbol{w}}_m$, and $\widetilde{\boldsymbol{w}}_s$ are the matrices and vectors of parameter estimation error, and they are defined as $\widetilde{\boldsymbol{W}}_m=\hat{\boldsymbol{W}}_m-\boldsymbol{W}_m$, $\widetilde{\boldsymbol{w}}_m=\hat{\boldsymbol{w}}_m-\boldsymbol{w}_m$, $\widetilde{\boldsymbol{W}}_s=\hat{\boldsymbol{W}}_s-\boldsymbol{W}_s$, and $\widetilde{\boldsymbol{w}}_s=\hat{\boldsymbol{w}}_s-\boldsymbol{w}_s$.

The time derivative of V_2 is described as

$$\dot{V}_2=(\dot{\boldsymbol{q}}_m-\dot{\boldsymbol{q}}_s)^T\boldsymbol{P}(\boldsymbol{q}_m-\boldsymbol{q}_s)=\dot{\boldsymbol{q}}_m^T\boldsymbol{P}(\boldsymbol{q}_m-\boldsymbol{q}_s)-\dot{\boldsymbol{q}}_s^T\boldsymbol{P}(\boldsymbol{q}_m-\boldsymbol{q}_s).\tag{A7}$$

Then there is

$$\begin{aligned}\dot{V}_1+\dot{V}_2\leq&-K_{m1}(\boldsymbol{q}_m-\boldsymbol{q}_s)^T(\boldsymbol{q}_m-\boldsymbol{q}_s)\boldsymbol{I}-\dot{\boldsymbol{q}}_m^T\boldsymbol{K}_m\dot{\boldsymbol{q}}_m+\dot{\boldsymbol{q}}_m^T\left(\widetilde{\boldsymbol{W}}_m^T\boldsymbol{\varphi}_m+\widetilde{\boldsymbol{w}}_m\right)\\&-\dot{\boldsymbol{q}}_m\boldsymbol{P}\int_{t-d_s}^{t}\dot{\boldsymbol{q}}_s(\xi)d\xi-2(\boldsymbol{q}_m-\boldsymbol{q}_s)^T\int_{t-d_s}^{t}\dot{\boldsymbol{q}}_s(\xi)d\xi\\&-K_{s1}(\boldsymbol{q}_s-\boldsymbol{q}_m)^T(\boldsymbol{q}_s-\boldsymbol{q}_m)\boldsymbol{I}-\dot{\boldsymbol{q}}_s^T\boldsymbol{K}_s\dot{\boldsymbol{q}}_s+\dot{\boldsymbol{q}}_s^T\left(\widetilde{\boldsymbol{W}}_s^T\boldsymbol{\varphi}_s+\widetilde{\boldsymbol{w}}_s\right)\\&-\dot{\boldsymbol{q}}_s^T\boldsymbol{P}\int_{t-d_m}^{t}\dot{\boldsymbol{q}}_m(\xi)d\xi-2(\boldsymbol{q}_s-\boldsymbol{q}_m)^T\int_{t-d_m}^{t}\dot{\boldsymbol{q}}_m(\xi)d\xi.\end{aligned}\tag{A8}$$

The time derivative of V_3 is

$$\begin{aligned}\dot{V}_3=&\bar{d}_m\dot{\boldsymbol{q}}_m^T\boldsymbol{Q}_m\dot{\boldsymbol{q}}_m-\int_{t-\bar{d}_m}^{t}\dot{\boldsymbol{q}}_m^T\boldsymbol{K}_m\dot{\boldsymbol{q}}_m dr+\bar{d}_s\dot{\boldsymbol{q}}_s^T\boldsymbol{Q}_s\dot{\boldsymbol{q}}_s-\int_{t-\bar{d}_s}^{t}\dot{\boldsymbol{q}}_s^T\boldsymbol{K}_s\dot{\boldsymbol{q}}_s dr\\\leq&\bar{d}_m\dot{\boldsymbol{q}}_m^T\boldsymbol{Q}_m\dot{\boldsymbol{q}}_m-\int_{t-d_m}^{t}\dot{\boldsymbol{q}}_m^T\boldsymbol{K}_m\dot{\boldsymbol{q}}_m dr+\bar{d}_s\dot{\boldsymbol{q}}_s^T\boldsymbol{Q}_s\dot{\boldsymbol{q}}_s-\int_{t-d_s}^{t}\dot{\boldsymbol{q}}_s^T\boldsymbol{K}_s\dot{\boldsymbol{q}}_s dr.\end{aligned}\tag{A9}$$

Sum $\dot{V}_1$, $\dot{V}_2$, and $\dot{V}_3$

$$\begin{aligned}
&\dot{V}_1+\dot{V}_2+\dot{V}_3\\
&\leq -K_{m1}(\boldsymbol{q}_m-\boldsymbol{q}_s)^T(\boldsymbol{q}_m-\boldsymbol{q}_s)\boldsymbol{I}-\dot{\boldsymbol{q}}_m^T\boldsymbol{K}_m\dot{\boldsymbol{q}}_m\\
&\quad+\dot{\boldsymbol{q}}_m^T\left(\widetilde{\boldsymbol{W}}_m^T\boldsymbol{\varphi}_m+\widetilde{\boldsymbol{w}}_m\right)+\bar{d}_m\dot{\boldsymbol{q}}_m^T\boldsymbol{Q}_m\dot{\boldsymbol{q}}_m\\
&\quad-\dot{\boldsymbol{q}}_m^T\boldsymbol{P}\int_{t-d_s}^{t}\dot{\boldsymbol{q}}_s d\xi-\lambda\int_{t-d_s}^{t}\dot{\boldsymbol{q}}_s^T\boldsymbol{Q}_s\dot{\boldsymbol{q}}_s dr\\
&\quad-2(\boldsymbol{q}_m-\boldsymbol{q}_s)^T\int_{t-d_s}^{t}\dot{\boldsymbol{q}}_s d\xi-(1-\lambda)\int_{t-d_s}^{t}\dot{\boldsymbol{q}}_s^T\boldsymbol{Q}_s\dot{\boldsymbol{q}}_s dr\\
&\quad-K_{s1}(\boldsymbol{q}_s-\boldsymbol{q}_m)^T(\boldsymbol{q}_s-\boldsymbol{q}_m)\boldsymbol{I}-\dot{\boldsymbol{q}}_s^T\boldsymbol{K}_s\dot{\boldsymbol{q}}_s\\
&\quad+\dot{\boldsymbol{q}}_s^T\left(\widetilde{\boldsymbol{W}}_s^T\boldsymbol{\varphi}_s+\widetilde{\boldsymbol{w}}_s\right)+\bar{d}_s\dot{\boldsymbol{q}}_s^T\boldsymbol{Q}_s\dot{\boldsymbol{q}}_s\\
&\quad-\dot{\boldsymbol{q}}_s^T\boldsymbol{P}\int_{t-d_m}^{t}\dot{\boldsymbol{q}}_m d\xi-\lambda\int_{t-d_m}^{t}\dot{\boldsymbol{q}}_m^T\boldsymbol{Q}_m\dot{\boldsymbol{q}}_m dr\\
&\quad-2(\boldsymbol{q}_s-\boldsymbol{q}_m)^T\int_{t-d_m}^{t}\dot{\boldsymbol{q}}_m d\xi-(1-\lambda)\int_{t-d_m}^{t}\dot{\boldsymbol{q}}_m^T\boldsymbol{Q}_m\dot{\boldsymbol{q}}_m dr.
\end{aligned}\tag{A10}$$

where $0<\lambda\leq 1$.

Considering Lemma 1, it can be obtained as

$$\begin{aligned}
&-\dot{\boldsymbol{q}}_m^T\boldsymbol{P}\int_{t-d_s}^{t}\dot{\boldsymbol{q}}_s d\xi-\lambda\int_{t-d_s}^{t}\dot{\boldsymbol{q}}_s^T\boldsymbol{Q}_s\dot{\boldsymbol{q}}_s dr\leq\frac{\bar{d}_s}{4\lambda}\dot{\boldsymbol{q}}_m^T\boldsymbol{P}\boldsymbol{Q}_s^{-1}\boldsymbol{P}^T\dot{\boldsymbol{q}}_m,\\
&-\dot{\boldsymbol{q}}_s^T\boldsymbol{P}\int_{t-d_m}^{t}\dot{\boldsymbol{q}}_m d\xi-\lambda\int_{t-d_m}^{t}\dot{\boldsymbol{q}}_m^T\boldsymbol{Q}_m\dot{\boldsymbol{q}}_m dr\leq\frac{\bar{d}_m}{4\lambda}\dot{\boldsymbol{q}}_s^T\boldsymbol{P}\boldsymbol{Q}_m^{-1}\boldsymbol{P}^T\dot{\boldsymbol{q}}_s,\\
&-2(\boldsymbol{q}_m-\boldsymbol{q}_s)^T\int_{t-d_s}^{t}\dot{\boldsymbol{q}}_s d\xi-(1-\lambda)\int_{t-d_s}^{t}\dot{\boldsymbol{q}}_s^T\boldsymbol{Q}_s\dot{\boldsymbol{q}}_s dr\\
&\leq\frac{\bar{d}_s}{1-\lambda}(\boldsymbol{q}_m-\boldsymbol{q}_s)^T\boldsymbol{Q}_s^{-1}\boldsymbol{B}_m^T(\boldsymbol{q}_m-\boldsymbol{q}_s)\\
&-2(\boldsymbol{q}_s-\boldsymbol{q}_m)^T\int_{t-d_m}^{t}\dot{\boldsymbol{q}}_m d\xi-(1-\lambda)\int_{t-d_m}^{t}\dot{\boldsymbol{q}}_m^T\boldsymbol{Q}_m\dot{\boldsymbol{q}}_m dr\\
&\leq\frac{\bar{d}_m}{1-\lambda}(\boldsymbol{q}_m-\boldsymbol{q}_s)^T\boldsymbol{Q}_m^{-1}\boldsymbol{B}_s^T(\boldsymbol{q}_m-\boldsymbol{q}_s)
\end{aligned}\tag{A11}$$

Based on the above inequality, the following results can be further obtained

$$\begin{aligned}
\dot{V}_1+\dot{V}_2+\dot{V}_3\leq&-(\boldsymbol{q}_m-\boldsymbol{q}_s)^T\boldsymbol{\Gamma}(\boldsymbol{q}_m-\boldsymbol{q}_s)\\
&-\dot{\boldsymbol{q}}_m^T\boldsymbol{\Psi}_m\dot{\boldsymbol{q}}_m+\dot{\boldsymbol{q}}_m^T\left(\widetilde{\boldsymbol{W}}_m^T\boldsymbol{\varphi}_m+\widetilde{\boldsymbol{w}}_m\right)\\
&-\dot{\boldsymbol{q}}_s^T\boldsymbol{\Psi}_s\dot{\boldsymbol{q}}_s+\dot{\boldsymbol{q}}_s^T\left(\widetilde{\boldsymbol{W}}_s^T\boldsymbol{\varphi}_s+\widetilde{\boldsymbol{w}}_s\right)
\end{aligned}\tag{A12}$$

where the gain matrices $\boldsymbol{\Gamma}$, $\boldsymbol{\Psi}_m$, and $\boldsymbol{\Psi}_s$ are defined as

$$\begin{aligned}
\boldsymbol{\Gamma}&=K_{m1}\boldsymbol{I}-\frac{\bar{d}_s}{1-\lambda}\boldsymbol{Q}_s^{-1}+K_{s1}\boldsymbol{I}-\frac{\bar{d}_m}{1-\lambda}bmQ_m^{-1}\\
\boldsymbol{\Psi}_m&=\boldsymbol{K}_m-\bar{d}_m\boldsymbol{Q}_m-\frac{\bar{d}_s}{4\lambda}\boldsymbol{P}\boldsymbol{Q}_s^{-1}\boldsymbol{P}^T\\
\boldsymbol{\Psi}_s&=\boldsymbol{K}_s-\bar{d}_s\boldsymbol{Q}_s-\frac{\bar{d}_m}{4\lambda}\boldsymbol{P}\boldsymbol{Q}_m^{-1}\boldsymbol{P}^T
\end{aligned}\tag{A13}$$

Based on the conditions set by the theorem, these matrices $\boldsymbol{\Gamma}$, $\boldsymbol{\Psi}_m$, and $\boldsymbol{\Psi}_s$ are all positive semidefinite.

With the adaptive laws in (10), the time derivative of V_4 is

$$\begin{aligned}\dot{V}_4 =& -\dot{\boldsymbol{q}}_m^T\widetilde{\boldsymbol{W}}_m^T\boldsymbol{\varphi}_m - \dot{\boldsymbol{q}}_m^T\widetilde{\boldsymbol{w}}_m - \frac{\Lambda_{m1}}{K_{m2}}\mathrm{tr}\left(\widetilde{\boldsymbol{W}}_m^T\widehat{\boldsymbol{W}}_m\right) - \frac{\Lambda_{m2}}{K_{m3}}\widetilde{\boldsymbol{w}}_m^T\widehat{\boldsymbol{w}}_m \\ & - \dot{\boldsymbol{q}}_s^T\widetilde{\boldsymbol{W}}_s^T\boldsymbol{\varphi}_s - \dot{\boldsymbol{q}}_s^T\widetilde{\boldsymbol{w}}_s - \frac{\Lambda_{s1}}{K_{s2}}\mathrm{tr}\left(\widetilde{\boldsymbol{W}}_s^T\widehat{\boldsymbol{W}}_s\right) - \frac{\Lambda_{s2}}{K_{s3}}\widetilde{\boldsymbol{w}}_s^T\widehat{\boldsymbol{w}}_s \\ \leq & -\dot{\boldsymbol{q}}_m^T\widetilde{\boldsymbol{W}}_m^T\boldsymbol{\varphi}_m - \frac{\Lambda_{m1}}{2K_{m2}}\mathrm{tr}\left(\widetilde{\boldsymbol{W}}_m^T\widetilde{\boldsymbol{W}}_m\right) + \frac{\Lambda_{m1}}{2K_{m2}}\mathrm{tr}\left(\boldsymbol{W}_m^T\boldsymbol{W}_m\right) \\ & - \dot{\boldsymbol{q}}_m^T\widetilde{\boldsymbol{w}}_m - \frac{\Lambda_{m2}}{2K_{m3}}\widetilde{\boldsymbol{w}}_m^T\widetilde{\boldsymbol{w}}_m + \frac{\Lambda_{m2}}{2K_{m3}}\boldsymbol{w}_m^T\boldsymbol{w}_m \\ & - \dot{\boldsymbol{q}}_s^T\widetilde{\boldsymbol{W}}_s^T\boldsymbol{\varphi}_s - \frac{\Lambda_{s1}}{2K_{s2}}\mathrm{tr}\left(\widetilde{\boldsymbol{W}}_s^T\widetilde{\boldsymbol{W}}_s\right) + \frac{\Lambda_{s1}}{2K_{s2}}\mathrm{tr}\left(\boldsymbol{W}_s^T\boldsymbol{W}_s\right) \\ & - \dot{\boldsymbol{q}}_s^T\widetilde{\boldsymbol{w}}_s - \frac{\Lambda_{s2}}{2K_{s3}}\widetilde{\boldsymbol{w}}_s^T\widetilde{\boldsymbol{w}}_s + \frac{\Lambda_{s2}}{2K_{s3}}\boldsymbol{w}_s^T\boldsymbol{w}_s\end{aligned} \tag{A14}$$

So

$$\begin{aligned}\dot{V} =& \dot{V}_1 + \dot{V}_2 + \dot{V}_3 + \dot{V}_4 \\ \leq & -(\boldsymbol{q}_m - \boldsymbol{q}_s)^T\boldsymbol{\Gamma}(\boldsymbol{q}_m - \boldsymbol{q}_s) - \dot{\boldsymbol{q}}_m^T\boldsymbol{\Psi}_m\dot{\boldsymbol{q}}_m - \dot{\boldsymbol{q}}_s^T\boldsymbol{\Psi}_s\dot{\boldsymbol{q}}_s \\ & - \frac{\Lambda_{m1}}{2K_{m2}}\mathrm{tr}\left(\widetilde{\boldsymbol{W}}_m^T\widetilde{\boldsymbol{W}}_m\right) - \frac{\Lambda_{m2}}{2K_{m3}}\widetilde{\boldsymbol{w}}_m^T\widetilde{\boldsymbol{w}}_m \\ & - \frac{\Lambda_{s1}}{2K_{s2}}\mathrm{tr}\left(\widetilde{\boldsymbol{W}}_s^T\widetilde{\boldsymbol{W}}_s\right) - \frac{\Lambda_{s2}}{2K_{s3}}\widetilde{\boldsymbol{w}}_s^T\widetilde{\boldsymbol{w}}_s + \Lambda\end{aligned} \tag{A15}$$

where Λ is a positive constant and defined as

$$\Lambda = \frac{\Lambda_{m1}}{2K_{m2}}\mathrm{tr}\left(\boldsymbol{W}_m^T\boldsymbol{W}_m\right) + \frac{\Lambda_{m2}}{2K_{m3}}\boldsymbol{w}_m^T\boldsymbol{w}_m + \frac{\Lambda_{s1}}{2K_{s2}}\mathrm{tr}\left(\boldsymbol{W}_s^T\boldsymbol{W}_s\right) + \frac{\Lambda_{s2}}{2K_{s3}}\boldsymbol{w}_s^T\boldsymbol{w}_s. \tag{A16}$$

Further considering $\dot{V}$, the following inequality relations are established

$$\begin{aligned}\dot{V} \leq & -\Omega_1\Big[(\boldsymbol{q}_m - \boldsymbol{q}_s)^T(\boldsymbol{q}_m - \boldsymbol{q}_s) + \dot{\boldsymbol{q}}_m^T\dot{\boldsymbol{q}}_m + \dot{\boldsymbol{q}}_s^T\dot{\boldsymbol{q}}_s \\ & + \mathrm{tr}\left(\widetilde{\boldsymbol{W}}_m^T\widetilde{\boldsymbol{W}}_m\right) + \widetilde{\boldsymbol{w}}_m^T\widetilde{\boldsymbol{w}}_m + \mathrm{tr}\left(\boldsymbol{W}_s^T\boldsymbol{W}_s\right) + \widetilde{\boldsymbol{w}}_s^T\widetilde{\boldsymbol{w}}_s\Big] + \Lambda\end{aligned} \tag{A17}$$

where Ω_1 is defined as

$$\Omega_1 = \min\left(\Gamma_{min}, \Psi_{m,min}, \Psi_{s,min}, \frac{\Lambda_{m1}}{2K_{m2}}, \frac{\Lambda_{m2}}{2K_{m3}}, \frac{\Lambda_{s1}}{2K_{s2}}, \frac{\Lambda_{s2}}{2K_{s3}}\right) \tag{A18}$$

where Γ_{min}, $\Psi_{m,min}$, and $\Psi_{s,min}$ are the minimum eigenvalues of matrices $\boldsymbol{\Gamma}$, $\boldsymbol{\Psi}_m$, and $\boldsymbol{\Psi}_s$, respectively.

From $\dot{\boldsymbol{q}}_j^T\boldsymbol{Q}_j\dot{\boldsymbol{q}}_j \leq Q_{j,max}\dot{\boldsymbol{q}}_j^T\dot{\boldsymbol{q}}_j$, $j = m, s$ and $Q_{j,max}$ being the smallest eigenvalue of $\boldsymbol{Q}_j$, we can obtain that

$$\int_{-\bar{d}_j}^{0}\int_{t+\theta}^{t}\dot{\boldsymbol{q}}_j^T(\xi)\boldsymbol{Q}_j\dot{\boldsymbol{q}}_j(\xi)d\xi d\theta \leq \frac{\bar{d}_j^2}{2}Q_{j,max}\dot{\boldsymbol{q}}_j^T\dot{\boldsymbol{q}}_j. \tag{A19}$$

Therefore, the derivative of the Lyapunov–Krasovskii function V can be written as follows

$$\begin{aligned}\dot{V} \leq & \Omega_2\Big[(\boldsymbol{q}_m - \boldsymbol{q}_s)^T(\boldsymbol{q}_m - \boldsymbol{q}_s) + \dot{\boldsymbol{q}}_m^T\dot{\boldsymbol{q}}_m + \dot{\boldsymbol{q}}_s^T\dot{\boldsymbol{q}}_s \\ & + \mathrm{tr}\left(\widetilde{\boldsymbol{W}}_m^T\widetilde{\boldsymbol{W}}_m\right) + \widetilde{\boldsymbol{w}}_m^T\widetilde{\boldsymbol{w}}_m + \mathrm{tr}\left(\boldsymbol{W}_s^T\boldsymbol{W}_s\right) + \widetilde{\boldsymbol{w}}_s^T\widetilde{\boldsymbol{w}}_s\Big]\end{aligned} \tag{A20}$$

where Ω_2 is a positive real number and is defined as

$$\Omega_2 = \max\left(\frac{M_{m,max} + \bar{d}_m^2Q_{m,max}}{2}, \frac{M_{s,max} + \bar{d}_s^2Q_{s,max}}{2}, \frac{P_{max}}{2}, \frac{\Lambda_{m1}}{2}, \frac{\Lambda_{m2}}{2}, \frac{\Lambda_{s1}}{2}, \frac{\Lambda_{s2}}{2}\right) \tag{A21}$$

$M_{m,max}$, $M_{s,max}$, P_{max}, $Q_{m,max}$, and $Q_{s,max}$ are the maximum eigenvalues of matrices of $\boldsymbol{M}_m$, $\boldsymbol{M}_s$, $\boldsymbol{P}$, $\boldsymbol{Q}_s$, and $\boldsymbol{Q}_s$, respectively.

Therefore, it is obvious that the following results can be obtained

$$\dot{V} \leq -\frac{\Omega_1}{\Omega_2} V + \Lambda. \tag{A22}$$

If the gain coefficient of the control laws in the theorem is satisfied, then it can get that Ω_1 is a positive real number. Based on Lemma 2, there exists a t_0 for $t > t_0 > 0$, we can get

$$\dot{V} \leq e^{-\frac{\Omega_1}{\Omega_2}(t-t_0)} V(t_0) + \frac{\Lambda\Omega_2}{\Omega_1}\left(1 - e^{-\frac{\Omega_1}{\Omega_2}(t-t_0)}\right) \tag{A23}$$

Then it can be further obtained that

$$\lim_{t\to\infty} V(t) \leq \frac{\Lambda\Omega_2}{\Omega_1}. \tag{A24}$$

It is obvious that the closed-loop system is stable and the Lyapunov–Krasovskii function V is bounded, which also means that the position error $\boldsymbol{q}_m - \boldsymbol{q}_s$ and velocities $\dot{\boldsymbol{q}}_m$ and $\dot{\boldsymbol{q}}_s$ are also bounded. This completes the proof. □

References

1. Soylu, S.; Firmani, F.; Buckham, B.J.; Podhorodeski, R.P. Comprehensive underwater vehicle-manipulator system teleoperation. In *Oceans 2010 MTS/IEEE Seattle*; IEEE: Piscataway, NJ, USA, 2010; pp. 1–8.
2. Wei, D.; Huang, B.; Li, Q. Multi-view merging for robot teleoperation with virtual reality. *IEEE Robot. Automat. Lett.* **2021**, *6*, 8537–8544.
3. Saltaren, R.; Aracil, R.; Alvarez, C.; Yime, E.; Sabater, J.M. Field and service applications-exploring deep sea by teleoperated robot-an underwater parallel robot with high navigation capabilities. *IEEE Robot. Automat. Mag.* **2007**, *14*, 65–75. [CrossRef]
4. Hokayem, P.F.; Spong, M.W. Bilateral teleoperation: An historical survey. *Automatica* **2006**, *42*, 2035–2057. [CrossRef]
5. Yang, Y.; Hua, C.C.; Li, J. A novel delay-dependent finite-time control of telerobotics system with asymmetric time-varying delays. *IEEE Trans. Control Syst. Technol.* **2022**, *30*, 985–996. [CrossRef]
6. Anderson, R.J.; Spong, M.W. Bilateral control of teleoperators with time delay. In Proceedings of the 1988 IEEE International Conference on Systems, Man, and Cybernetics, Beijing, China, 8–12 August 1988; pp. 131–138.
7. Chen, H.C.; Liu, Y.C. Passivity-based control framework for task-space bilateral teleoperation with parametric uncertainty over unreliable networks. *ISA Trans.* **2017**, *70*, 187–199.
8. Chen, Z.; Huang, F.; Song, W.; Zhu, S. A novel wave-variable based time-delay compensated four-channel control design for multilateral teleoperation system. *IEEE Access* **2018**, *6*, 25506–25516. [CrossRef]
9. Sun, D.; Naghdy, F.; Du, H. Application of wave-variable control to bilateral teleoperation systems: A survey. *Annu. Rev. Control* **2014**, *38*, 12–31. [CrossRef]
10. Yang, C.; Wang, X.; Li, Z. Teleoperation control based on combination of wave variable and neural networks. *IEEE Trans. Syst. Man Cybern. Syst.* **2017**, *47*, 2125–2136. [CrossRef]
11. Huang, P.; Dai, P.; Lu, Z. Asymmetric wave variable compensation method in dual-master-dual-slave multilateral teleoperation system. *Mechatronics* **2018**, *49*, 1–10.
12. Al-Wais, S.; Khoo, S.; Lee, T.H.; Shanmugam, L.; Nahavandi, S. Robust H cost guaranteed integral sliding mode control for the synchronization problem of nonlinear tele-operation system with variable time-delay. *ISA Trans.* **2018**, *72*, 25–36. [CrossRef]
13. Wang, H.; Liu, P.X.; Liu, S. Adaptive neural synchronization control for bilateral teleoperation systems with time delay and backlash-like hysteresis. *IEEE Trans. Cybern.* **2017**, *47*, 3018–3026. [PubMed]
14. Chen, Z.; Huang, F.; Sun, W.; Gu, J.; Yao, B. RBF-neural-network-based adaptive robust control for nonlinear bilateral teleoperation manipulators with uncertainty and time delay. *IEEE/ASME Trans. Mechatronics* **2020**, *25*, 906–918. [CrossRef]
15. Yang, L.; Chen, Y.; Liu, Z.; Chen, K.R.; Zhang, Z.X. Adaptive fuzzy control for teleoperation system with uncertain kinematics and dynamics. *Internat J. Control Automat. Syst.* **2019**, *17*, 1158–1166. [CrossRef]
16. Kebria, P.; Khosravi, A.; Nahavandi, S.; Wu, D.; Bello, F. Adaptive type-2 fuzzy neural-network control for teleoperation systems with delay and uncertainties. *IEEE Trans. Fuzzy Sys.* **2020**, *28*, 2543–2554.
17. Yang, Y.N.; Hua, C.C.; Li, J.P. Composite adaptive guaranteed performances synchronization control for bilateral teleoperation system with asymmetrical time-varying delays. *IEEE Trans. Cybern.* **2022**, *52*, 5486–5497. [CrossRef]
18. Zhao, L.; Zhang, H.; Yang, Y.; Yang, H. Integral sliding mode control of a bilateral teleoperation system based on extended state observers. *Internat J. Control Automat. Syst.* **2017**, *15*, 2118–2125. [CrossRef]

19. Chen, Z.; Huang, F.; Chen, W.; Zhang, J.; Sun, W.; Chen, J.; Gu, J.; Zhu, S. RBFNN-based adaptive sliding mode control design for delayed nonlinear multilateral telerobotic system with cooperative manipulation. *IEEE Trans. Industr. Inform.* **2020**, *16*, 1236–1247. [CrossRef]
20. Zhang, H.; Song, A.; Li, H.; Shen, S. Novel adaptive finite time control of teleoperation system with time-varying delays and input saturation. *IEEE Trans. Cybern.* **2021**, *57*, 3724–3737. [CrossRef]
21. Hua, C.C.; Yang, Y.; Liu, P.X. Output-feedback adaptive control of networked teleoperation system with time-varying delay and bounded inputs. IEEE/ASME Trans. *Mechatronics* **2014**, *20*, 2009–2020.
22. Kostyukova, O.; Vista IV, F.P.; Chong, K.T. Design of feedforward and feedback position control for passive bilateral teleoperation with delays. *ISA Trans.* **2019**, *85*, 200–213. [CrossRef]
23. Shen, S.; Song, A.; Li, H.; Li, T. Constrained control for cloud robotic under time delay based on command governor with interval estimation. *IEEE Access* **2019**, *7*, 70999–71006.
24. Nuño, E.; Ortega, R.; Barabanov, N.; Basañez, L. A globally stable PD controller for bilateral teleoperators. *IEEE Trans. Robot.* **2008**, *24*, 753–758. [CrossRef]
25. Nuño, E.; Basañez, L.; López-Franco, C. Arana-Daniel, N. Stability of nonlinear teleoperators using PD controllers without velocity measurements. *J. Frankl. Inst.* **2014**, *351*, 241–258. [CrossRef]
26. Slawinski, E.; Mut, V. PD-like controllers for delayed bilateral teleoperation of manipulators robots. *Internat J. Robust Nonlinear Control* **2015**, *25*, 1801–1815. [CrossRef]
27. Islam, S.; Liu, X.P.P.; El-Saddik, A. Teleoperation systems with symmetric and unsymmetric time varying communication delay. *IEEE Trans. Instrum. Meas.* **2013**, *62*, 2943–2953.
28. Hashemzadeh, F.; Tavakoli, M. Position and force tracking in nonlinear teleoperation systems under varying delays. *Robotics* **2015**, *33*, 1003–1016.
29. Chan, L.P.; Naghdy, F.; Stirling, D. Position and force tracking for non-linear haptic tele-manipulator under varying delays with an improved extended active observer. *Robot. Auton. Syst.* **2016**, *75*, 145–160.
30. Ganjefar, S.; Rezaei, S.; Hashemzadeh, F. Position and force tracking in nonlinear teleoperation systems with sandwich linearity in actuators and time-varying delay. *Mech. Syst. Signal Pr.* **2017**, *86*, 308–324.
31. Deka, S.A.; Stipanovic, D.M.; Kesavadas, T. Stable bilateral teleoperation with bounded control. *IEEE Trans. Control Syst. Technol.* **2019**, *27*, 2351–2360. [CrossRef]
32. Zakerimanesh, A.; Sharifi, M.; Hashemzadeh, F.; Tavakoli, M. Delay-robust nonlinear control of bounded-input telerobotic systems with synchronization enhancement. *IEEE Robot. Automat. Lett.* **2021**, *6*, 2493–2500. [CrossRef]
33. Yang, Y.; Constantinescu, D.; Shi, Y. Input-to-state stable bilateral teleoperation by dynamic interconnection and damping injection: Theory and experiments. *IEEE Trans. Ind. Electron.* **2020**, *67*, 790–799.
34. De Lima, M.V.; Mozelli, L.A.; Neto, A.A.; Souza, F.O. A simple algebraic criterion for stability of bilateral teleoperation systems under time-varying delays. *Mech. Syst. Signal Pr.* **2020**, *137*, 106217. [CrossRef]
35. Hua, C.C.; Yang, Y.N. Bilateral teleoperation design with without gravity measurement. *IEEE Trans. Instrum. Meas.* **2012**, *61*, 3136–3146. [CrossRef]
36. Sarras, I.; Nuño, E.; Basañez, L. An adaptive controller for nonlinear teleoperators with variable time-delays. *J. Frankl. Inst.* **2014**, *351*, 4817–4837. [CrossRef]
37. Liu, Y.C.; Khong, M.H. Adaptive control for nonlinear teleoperators with uncertain kinematics and dynamics. *IEEE/ASME Trans. Mechatronics* **2015**, *20*, 2550–2562. [CrossRef]
38. Pourseifi, M.; Rezaei, S. Adaptive control for position and force tracking of uncertain teleoperation with actuators saturation and asymmetric varying time delays. *Internat J. Nonlin. Sci. Num.* **2022** , 1–20. [CrossRef]
39. Lu, Z.Y.; Guan, Y.; Wang, N. An adaptive fuzzy control for human-in-the-loop operations with varying communication time delays. *IEEE Robot. Automat. Lett.* **2022**, *7*, 5599–5606.
40. Spong, M.W.; Hutchinson, S.; Vidyasagar, M. *Robot Modeling and Control*; Wiley: New York, NY, USA, 2006; Volume 3.
41. Li, Z.; Xia, Y.; Su, C.Y. *Intelligent Networked Teleoperation Control*; Springer: Berlin, Germany, 2015.
42. Seshagiri, S.; Khalil, H.K. Output feedback control of nonlinear systems using RBF neural networks. *IEEE Trans. Neural Netw.* **2000**, *11*, 69–79. [CrossRef]
43. Nuño, E.; Basañez, L.; Ortega, R.; Spong, M. Position tracking for non-linear teleoperators with variable time delay. *Int. J. Robot. Res.* **2009**, *28*, 895–910.
44. Yang, Y.; Constantinescu, D.; Shi, Y. Robust four-channel teleoperation through hybrid damping-stiffness adjustment. *IEEE Trans. Control Syst. Technol.* **2020**, *28*, 920–935. [CrossRef]
45. Gong, Y.L.; Ji, Y.D. A novel passivity criterion for bilateral teleoperation under event triggered PD-like control with constant time delays. *Intern. J. Control Automat. Syst.* **2022**, *20*, 2353–2363. [CrossRef]
46. Hua, C.C.; Liu, X.P. Delay-dependent stability criteria of teleoperation systems with asymmetric time-varying delays. *IEEE Trans. Robot.* **2010**, *26*, 925–932. [CrossRef]
47. Liu, X.K. *Robot Control System Design and Matlab Simulation: The Basic Design Method*; Tsinghua University Press: Beijing, China, 2016.